

All tree-level amplitudes in massless QCD

LANCE J. DIXON,

*Theory Group, Physics Department,
CERN, CH-1211 Geneva 23, Switzerland*

and

*SLAC National Accelerator Laboratory,
Stanford University, Stanford, CA 94309, USA
lance@slac.stanford.edu*

JOHANNES M. HENN, JAN PLEFKA AND THEODOR SCHUSTER

*Institut für Physik, Humboldt-Universität zu Berlin,
Newtonstraße 15, D-12489 Berlin, Germany*

`{henn,plefka,theodor}@physik.hu-berlin.de`

Abstract

We derive compact analytical formulae for all tree-level color-ordered gauge theory amplitudes involving any number of external gluons and up to four massless quark-anti-quark pairs. A general formula is presented based on the combinatorics of paths along a rooted tree and associated determinants. Explicit expressions are displayed for the next-to-maximally helicity violating (NMHV) and next-to-next-to-maximally helicity violating (NNMHV) gauge theory amplitudes. Our results are obtained by projecting the previously-found expressions for the super-amplitudes of the maximally supersymmetric super Yang-Mills theory ($\mathcal{N} = 4$ SYM) onto the relevant components yielding all gluon-gluino tree amplitudes in $\mathcal{N} = 4$ SYM. We show how these results carry over to the corresponding QCD amplitudes, including massless quarks of different flavors as well as a single electroweak vector boson. The public `Mathematica` package `GGT` is described, which encodes the results of this work and yields analytical formulae for all $\mathcal{N} = 4$ SYM gluon-gluino trees. These in turn yield all QCD trees with up to four external arbitrary-flavored massless quark-anti-quark pairs.

Contents

1	Introduction and conclusions	2
2	Color-ordering and spinor-helicity formalism	5
3	From $\mathcal{N} = 4$ SYM to QCD tree amplitudes	6
4	All gluon tree amplitudes	13
5	All single-flavor quark-anti-quark-gluon trees	16
6	All gluon-gluino tree amplitudes in $\mathcal{N} = 4$ super Yang-Mills	19
7	Proof of the master formula	19
A	Explicit formulae for gluon trees	23
A.1	NMHV amplitudes	24
A.2	N ² MHV amplitudes	24
B	Explicit formulae for trees with fermions	26
B.1	MHV amplitudes	26
B.2	NMHV amplitudes	27
B.3	N ² MHV amplitudes	34
C	The Mathematica package GGT	36

1 Introduction and conclusions

Scattering amplitudes play a central role in gauge theory. At a phenomenological level, they are critical to the prediction of cross sections at high-energy colliders, for processes within and beyond the Standard Model. Efficient evaluation of scattering amplitudes involving many quarks and gluons is particularly important at machines such as the Large Hadron Collider (LHC), in which complex, multi-jet final states are produced copiously and complicate the search for new physics.

Tree amplitudes can be used to predict cross sections at leading order (LO) in the perturbative expansion in the QCD coupling α_s . Such results are already available numerically for a wide variety of processes. Programs such as MADGRAPH [1], COMPHEP [2], and AMEGIC++ [3]

are based on fast numerical evaluation of Feynman diagrams. Other methods include the Berends-Giele (off shell) recursion relations [4], as implemented for example in COMIX [5], and the related ALPHA [6] and HELAC [7] algorithms based on Dyson-Schwinger equations, as well as O'MEGA/WHIZARD [8]. The computation time required in these latter methods scales quite well with the number of legs.

On the formal side, the properties of scattering amplitudes have long provided numerous clues to hidden symmetries and dynamical structures in gauge theory. It was recognized early on that tree amplitudes in gauge theory are effectively supersymmetric [9], so that they obey supersymmetric S -matrix Ward identities [10]. Soon thereafter, Parke and Taylor [11] discovered a remarkably simple formula for the maximally-helicity-violating (MHV) amplitudes for n -gluon scattering, which was proven by Berends and Giele [4], and soon generalized to $\mathcal{N} = 4$ super Yang-Mills theory (SYM) by Nair [12].

Later, it was found that this simplicity also extends to the loop level, at least for $\mathcal{N} = 4$ super Yang-Mills theory [13, 14]. These results were obtained using the unitarity method, which constructs loop amplitudes by sewing together tree amplitudes (for recent reviews see refs. [15]). After Witten [16] reformulated gauge theory in terms of a topological string propagating in twistor space, there was a huge resurgence of interest in uncovering new properties of scattering amplitudes and developing new methods for their efficient computation. Among other developments, Britto, Cachazo, Feng and Witten proved a new type of recursion relation [17] for gauge theory. In contrast to the earlier off-shell recursion relations, the BCFW relation uses only on-shell lower-point amplitudes, evaluated at complex momenta. A particular solution to this recursion relation was found for an arbitrary number of gluons in the split-helicity configuration $(-\cdots-+\cdots+)$ [18].

The BCFW recursion relation was then recast as a super-recursion relation for the tree amplitudes of $\mathcal{N} = 4$ super Yang-Mills theory, which involves shifts of Grassmann parameters as well as momenta [19]. A related construction is given in ref. [20]. The super-recursion relation of ref. [19] was solved for arbitrary external states by Drummond and one of the present authors [21]. Tree-level super-amplitudes have a dual superconformal invariance [22, 23], and the explicit solution does indeed have this symmetry [21]. It is written in terms of dual superconformal invariants, which are a straightforward generalization of those that first appeared in next-to-MHV (NMHV) super-amplitudes [22, 24]. This dual superconformal invariance of tree-level amplitudes is a hallmark of the integrability of planar $\mathcal{N} = 4$ SYM, as it closes with the standard superconformal symmetry into an infinite-dimensional symmetry of Yangian type [25] (a recent review is ref. [26]).

The purpose of this paper is to illustrate how these more recent formal developments can reap benefits for phenomenological applications in QCD. In particular, we will evaluate the solution in ref. [21] by carrying out the integrations over Grassmann parameters that are needed to select particular external states. In addition, we will show how to extract tree-level QCD amplitudes from the amplitudes of $\mathcal{N} = 4$ super Yang-Mills theory. While this extraction is simple for pure-gluon amplitudes, and those with a single massless quark line, it becomes a bit more intricate for amplitudes with multiple quark lines of different flavors, because of the need to forbid the exchange of scalar particles, which are present in $\mathcal{N} = 4$ super Yang-Mills theory but not in

QCD.

Although, as mentioned above, there are currently many numerical programs available for computing tree amplitudes efficiently, the existence of analytic expressions may provide a yet more efficient approach in some contexts. In fact, the formulae provided in this paper have already served a practical purpose: They were used to evaluate contributions from real emission in the NLO corrections to the cross section for producing a W boson in association with four jets at the LHC [27]. This process forms an important background to searches for various kinds of new physics, including supersymmetry. The real-emission corrections require evaluating nine-point tree amplitudes at a large number of different phase-space points (on the order of 10^8), in order to get good statistical accuracy for the Monte Carlo integration over phase space.

In principle, QCD tree amplitudes can also be used to speed up the evaluation of one-loop amplitudes, when the latter are constructed from tree amplitudes using a numerical implementation of generalized unitarity. Many different generalized unitarity cuts, and hence many different tree amplitudes, are involved in the construction of a single one-loop amplitude. The tree amplitudes described here enter directly into the construction of the “cut-constructible” part [14] of one-loop amplitudes in current programs such as CUTTOOLS [28], ROCKET [29,30] and BLACKHAT [31]. On the other hand, the computation-time bottleneck in these programs often comes from the so-called “rational” terms. When these terms are computed using only unitarity, it is via unitarity in D dimensions [32,30,33], not four dimensions. The amplitudes presented here are four-dimensional ones, so they cannot be used directly to alleviate this bottleneck for the D -dimensional unitarity method. However, in the numerical implementation of loop-level on-shell recursion relations [34] for the rational part in BLACKHAT [31], or in the OPP method used in CUTTOOLS [28], there are no D -dimensional trees, so this is not an issue.

An interesting avenue for future research would be to try to generalize the results presented in this paper to QCD amplitudes containing massive quarks, or other massive colored states. Massive quark amplitudes are of interest because, for example, processes that produce top quarks in association with additional jets can form important backgrounds to new physics at the LHC. States in $\mathcal{N} = 4$ SYM can be given masses through a super-Higgs mechanism. This mechanism was explored recently in the context of infrared regulation of $\mathcal{N} = 4$ SYM loop amplitudes [35]. However, it should be possible to generate the appropriate tree amplitudes with massive quarks, or other massive states, from the same kind of setup, once one solves the appropriate super-BCFW recursion relations.

The remainder of this paper is organized as follows. After introducing the standard technology of color-ordered amplitudes and spinor helicity we explain the strategies of how to extract QCD tree amplitudes with massless quarks from $\mathcal{N} = 4$ SYM in section 3. We also discuss how to convert these amplitudes into trees with one electroweak vector boson. Sections 4 through 6 are devoted to stating the general analytical formulae for gluon-gluino n -parton amplitudes in $\mathcal{N} = 4$ SYM, which are proven in section 7. In appendix A we provide a collection of explicit results for pure-gluon trees. Explicit formulae for trees involving up to six fermions are displayed in appendix B. Finally, appendix C is devoted to a documentation of our `Mathematica` package GGT which implements all of the results of this paper and yields the analytical expressions for an arbitrary flavored gluon-gluino tree amplitude in $\mathcal{N} = 4$ SYM. The package is included in the `arXiv.org`

2 Color-ordering and spinor-helicity formalism

Tree-level gluon amplitudes in non-abelian gauge theories may be conveniently separated into a sum of terms, each composed of a simple prefactor containing the color indices, multiplied by a kinematical factor known as a partial or color-ordered amplitude. For an n -gluon amplitude one has

$$\mathcal{A}_n^{\text{tree}}(\{p_i, h_i, a_i\}) = g^{n-2} \sum_{\sigma \in \mathcal{S}_n/Z_n} \text{Tr}(T^{a_{\sigma(1)}} \dots T^{a_{\sigma(n)}}) A_n(\sigma(1)^{h_{\sigma(1)}} \dots \sigma(n)^{h_{\sigma(n)}}), \quad (2.1)$$

with the argument i^{h_i} of the partial amplitude A_n denoting an outgoing gluon of light-like momentum p_i and helicity $h_i = \pm 1$, $i \in [1, n]$. The $su(N_c)$ generator matrices T^{a_i} are in the fundamental representation, and are normalized so that $\text{Tr}(T^a T^b) = \delta^{ab}$.

Color-ordered amplitudes of massless particles are most compactly expressed in the spinor-helicity formalism. Here all four-momenta are written as bi-spinors via

$$\not{p}^{\alpha\dot{\alpha}} = \sigma_{\mu}^{\alpha\dot{\alpha}} p^{\mu}, \quad (2.2)$$

where we take $\sigma^{\mu} = (\mathbf{1}, \vec{\sigma})$ with $\vec{\sigma}$ being the 2×2 Pauli spin matrices. Light-like vectors are then expressed via the product of two spinors

$$\not{p}^{\alpha\dot{\alpha}} = \lambda^{\alpha} \tilde{\lambda}^{\dot{\alpha}}. \quad (2.3)$$

For real momenta with Lorentz signature we have $\tilde{\lambda} = \pm \lambda^*$, with the sign being determined by the energy component of p . For complex momenta the spinors λ and $\tilde{\lambda}$ are independent. Our convention is such that all gluons are outgoing. Then in eq. (2.1) each color-ordered leg is specified by a choice of spinors λ_i and $\tilde{\lambda}_i$ along with a helicity $h_i = \pm 1$. Given this data the associated polarization vectors may be reconstructed from the expressions

$$\epsilon_{+,i}^{\alpha\dot{\alpha}} = \frac{\tilde{\lambda}_i^{\dot{\alpha}} \mu_i^{\alpha}}{\langle \lambda_i \mu_i \rangle}, \quad \epsilon_{-,i}^{\alpha\dot{\alpha}} = \frac{\lambda_i^{\alpha} \tilde{\mu}_i^{\dot{\alpha}}}{[\lambda_i \mu_i]}, \quad (2.4)$$

where $\mu_i^{\alpha} \tilde{\mu}_i^{\dot{\alpha}}$ are auxiliary momenta and we use the standard notation $\langle \lambda \mu \rangle = \epsilon_{\alpha\beta} \lambda^{\alpha} \mu^{\beta}$ and $[\lambda \mu] = \epsilon_{\dot{\alpha}\dot{\beta}} \lambda^{\dot{\alpha}} \mu^{\dot{\beta}}$. Moreover we shall often use the abbreviated forms $\langle ij \rangle = \langle \lambda_i \lambda_j \rangle$ and $[ij] = [\tilde{\lambda}_i \tilde{\lambda}_j]$ in the sequel. As an essential building block of the general tree-level scattering formula we introduce the dual coordinates or region momenta $x_{ij}^{\alpha\dot{\alpha}}$ via

$$x_{ij}^{\alpha\dot{\alpha}} := (\not{p}_i + \not{p}_{i+1} + \dots + \not{p}_{j-1})^{\alpha\dot{\alpha}} = \sum_{k=i}^{j-1} \lambda_k^{\alpha} \tilde{\lambda}_k^{\dot{\alpha}}, \quad i < j, \quad (2.5)$$

$x_{ii} = 0$, and $x_{ij} = -x_{ji}$ for $i > j$. We then define the scalar quantities

$$\langle na_1 a_2 \dots a_k | a \rangle := \langle n | x_{na_1} x_{a_1 a_2} \dots x_{a_{k-1} a_k} | a \rangle, \quad (2.6)$$

which we will use frequently in the following. In fact all amplitudes can be expressed in terms of the quantities $\langle na_1 a_2 \dots a_k | a \rangle$ and the spinor products $\langle i j \rangle$.

As an example of the notation and in order to give a flavor of the kinds of results we obtain, we present a compact formula for the n -point NMHV pure gluon amplitude in QCD

$$A_n^{\text{NMHV}}(i_1, i_2, n) = \frac{\delta^{(4)}(p)}{\langle 1 2 \rangle \dots \langle n 1 \rangle} \times \left[\sum_{i_1 < s \leq i_2 < t \leq n-1} \tilde{R}_{n;st} \left(\langle n i_1 \rangle \langle nts | i_2 \rangle \right)^4 + \sum_{i_1 < s < t \leq i_2} \tilde{R}_{n;st} \left(\langle i_2 n \rangle \langle n i_1 \rangle x_{st}^2 \right)^4 \right. \\ \left. + \sum_{2 \leq s \leq i_1 < i_2 < t \leq n-1} \tilde{R}_{n;st} \left(\langle i_2 i_1 \rangle \langle nts | n \rangle \right)^4 + \sum_{2 \leq s \leq i_1 < t \leq i_2} \tilde{R}_{n;st} \left(\langle n i_2 \rangle \langle nst | i_1 \rangle \right)^4 \right]. \quad (2.7)$$

Here i_1, i_2 and n correspond to the positions of the three negative-helicity gluons. (Using cyclic symmetry, we have put one of them at position n without loss of generality.) The quantities $\tilde{R}_{n;st}$ are simply given by

$$\tilde{R}_{n;st} := \frac{1}{x_{st}^2} \frac{\langle s(s-1) \rangle}{\langle nts | s \rangle \langle nts | s-1 \rangle} \frac{\langle t(t-1) \rangle}{\langle nst | t \rangle \langle nst | t-1 \rangle}. \quad (2.8)$$

with $\tilde{R}_{n;st} := 0$ for $t = s + 1$ or $s = t + 1$. Note that the above formula is given for an arbitrary number of gluons n . In realistic cases this number is usually small, say of the order of 9, in which case relatively few terms are produced by the nested sums in eq. (2.7).

3 From $\mathcal{N} = 4$ SYM to QCD tree amplitudes

In this section we discuss how to assign quantum numbers for external states in $\mathcal{N} = 4$ SYM in order to generate tree amplitudes for QCD with massless quarks. We then discuss the generation of tree amplitudes including an electroweak vector boson (W , Z or virtual photon). From the point of view of tree amplitudes, there are two principal differences between $\mathcal{N} = 4$ SYM and massless QCD. First of all, the fermions in $\mathcal{N} = 4$ SYM, the gluinos, are in the adjoint representation of $su(N_c)$, rather than the fundamental representation, and come in four flavors. Secondly, the $\mathcal{N} = 4$ SYM theory contains six massless scalars in the adjoint representation.

Because we use color-ordered amplitudes, as discussed in Sec. 2, the first difference is fairly unimportant. Quark amplitudes can be assembled from the same color-ordered amplitudes as gluino amplitudes, weighted with different color factors. For example, the color decomposition for amplitudes with a single quark-anti-quark pair, and the remaining $(n-2)$ partons gluons is,

$$\mathcal{A}_n^{\text{tree}}(1_{\bar{q}}, 2_q, 3, \dots, n) = g^{n-2} \sum_{\sigma \in S_{n-2}} (T^{a_{\sigma(3)}} \dots T^{a_{\sigma(n)}})_{i_2}^{\bar{i}_1} A_n^{\text{tree}}(1_{\bar{q}}, 2_q, \sigma(3), \dots, \sigma(n)). \quad (3.1)$$

The color-ordered amplitudes appearing in eq. (3.1) are just the subset of two-gluino- $(n-2)$ -gluon amplitudes in which the two gluinos are adjacent.

Amplitudes with more quark-anti-quark pairs have a somewhat more intricate color structure involving multiple strings of T^a matrices, as explained in ref. [36]. In this case, some of the color factors also include explicit factors of $1/N_c$, as required to project out the $su(N_c)$ -singlet state for gluon exchange between two different quark lines. However, all of the required kinematical coefficients can still be constructed from suitable linear combinations of the color-ordered amplitudes for $2k$ external gluinos and $(n - 2k)$ external gluons.

The main goal of this section will be to illustrate how to choose the flavors of the external gluinos in order to accomplish two things: (1) avoid the internal exchange of massless scalars, and (2) allow all fermion lines present to be for distinct flavors. (In some cases one may want amplitudes with (partially) identical fermions; these can always be constructed from the distinct-flavor case by summing over the relevant exchange-terms, although it may be more efficient to compute the identical-fermion case directly.) We will accomplish this goal for amplitudes containing up to four separate fermion lines, that is, eight external fermion states.

In gauge theory, tree amplitudes that contain only external gluons are independent of the matter states in the theory [9]; hence they are identical between $\mathcal{N} = 4$ SYM and QCD. The reason is simply that the vertices that couple gluons to the other states in the theory always produce the fermions and scalars in pairs. There are no vertices that can destroy all the fermions and scalars, once they have been produced. If a fermion or scalar were produced at any point in a tree diagram, it would have to emerge from the diagram, which would no longer have only external gluons. In other words, the pure-gluon theory forms a closed subsector of $\mathcal{N} = 4$ SYM.

Another closed subsector of $\mathcal{N} = 4$ SYM is $\mathcal{N} = 1$ SYM, which contains a gluon and a single gluino. Let g denote the gluon, \tilde{g}_A , $A = 1, 2, 3, 4$, denote the four gluinos, and $\phi_{AB} = -\phi_{BA}$ denote the six real scalars of $\mathcal{N} = 4$ SYM. Then the $\mathcal{N} = 1$ SYM subsector is formed by (g, \tilde{g}_1) . The reason it is closed is similar to the pure-gluon case just discussed: There are vertices that produce states other than (g, \tilde{g}_1) , but they always do so in pairs. For example, the Yukawa coupling $\phi^{AB}\tilde{g}_A\tilde{g}_B$, $A \neq B$, can convert \tilde{g}_1 into a scalar and a gluino each carrying an index $B \neq 1$. However, this index cannot be destroyed by further interactions.

The fact that $\mathcal{N} = 1$ SYM forms a closed subsector of $\mathcal{N} = 4$ SYM, in addition to color ordering, immediately implies that any color-ordered QCD tree amplitude for gluons, plus arbitrarily many quarks of a single flavor, is given directly by the corresponding amplitude (with \tilde{g}_1 replacing the single quark flavor) evaluated in $\mathcal{N} = 4$ SYM. The less trivial QCD amplitudes to extract are those for multiple fermion flavors, primarily because of the potential for intermediate scalar exchange induced by the Yukawa coupling $\phi^{AB}\tilde{g}_A\tilde{g}_B$. Figure 1 illustrates scalar exchange in an amplitude with four fermions belonging to two different flavor lines, $A \neq B$.

The key to avoiding such unwanted scalar exchange is provided by figure 2, which shows four types of vertices that could potentially couple fermion pairs to scalars and gluons. However, all four types of vertices vanish. (Recall that helicities are labeled in an all-outgoing convention.) Case (a) vanishes because the Yukawa interaction only couples gluinos of different flavors, $A \neq B$. Cases (b) and (c) vanish because of fermion helicity conservation for the gauge interactions, and a helicity flip for the Yukawa coupling. Case (d) vanishes because gluon interactions do not change flavor.

Because the emission of gluons from fermions does not change their helicity or flavor, in

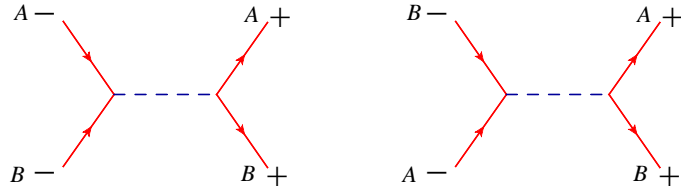


Figure 1: Unwanted scalar exchange between fermions of different flavors, $A \neq B$.

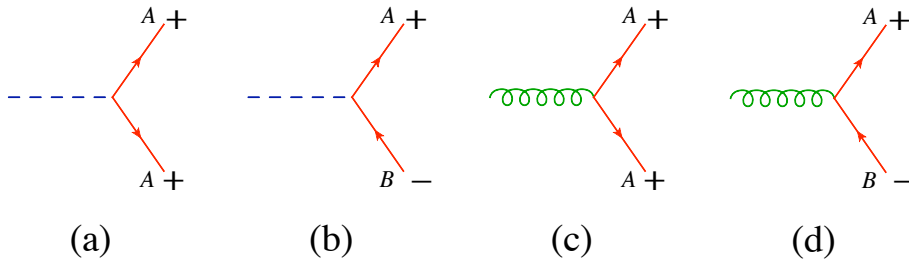


Figure 2: These vertices all vanish, as explained in the text. This fact allows us to avoid scalar exchange and control the flow of fermion flavor.

analyzing whether scalar exchange can be avoided, as well as the pattern of fermion flavor flow, one can ignore the gluons altogether. For example, figure 3 shows the possible cases for amplitudes with one or two fermion lines. The left-hand side of the equality shows the desired (color-ordered) fermion-line flow and helicity assignment for a QCD tree amplitude. All gluons have been omitted, and all fermion lines on the left-hand side are assumed to have distinct flavors. The right-hand side of the equality displays a choice of gluino flavor that leads to the desired amplitude. All other one- and two-fermion-line cases are related to the ones shown by parity or cyclic or reflection symmetries.

The one-fermion line, case (1), is trivial because $\mathcal{N} = 1$ SYM forms a closed subsector of $\mathcal{N} = 4$ SYM. In case (2a) we must choose all gluinos to have the same flavor; otherwise a scalar would be exchanged in the horizontal direction. Here, helicity conservation prevents the exchange of an unwanted gluon in this direction, keeping the two flavors distinct as desired. In case (2b), we must use two different gluino flavors, as shown; otherwise helicity conservation would allow gluon exchange in the wrong channel, corresponding to identical rather than distinct quarks.

More generally, in order to avoid scalar exchange, if two color-adjacent gluinos have the same helicity, then we should choose them to have the same flavor. In other words, we should forbid all configurations of the form (\dots, A^+, B^+, \dots) and (\dots, A^-, B^-, \dots) for $A \neq B$, where A^\pm stands for the gluino state \tilde{g}_A^\pm . While this is necessary, it is not sufficient. For example, we also need to forbid configurations such as $(\dots, A^+, C^\pm, C^\mp, B^+, \dots)$, because the pair (C^\pm, C^\mp) could be produced by a gluon splitting into this pair, which also connects to the (A^+, B^+) fermion line. As a secondary consideration, if two color-adjacent gluinos have opposite helicity, then we should choose them to have the same flavor or different flavor according to the desired quark flavor flow

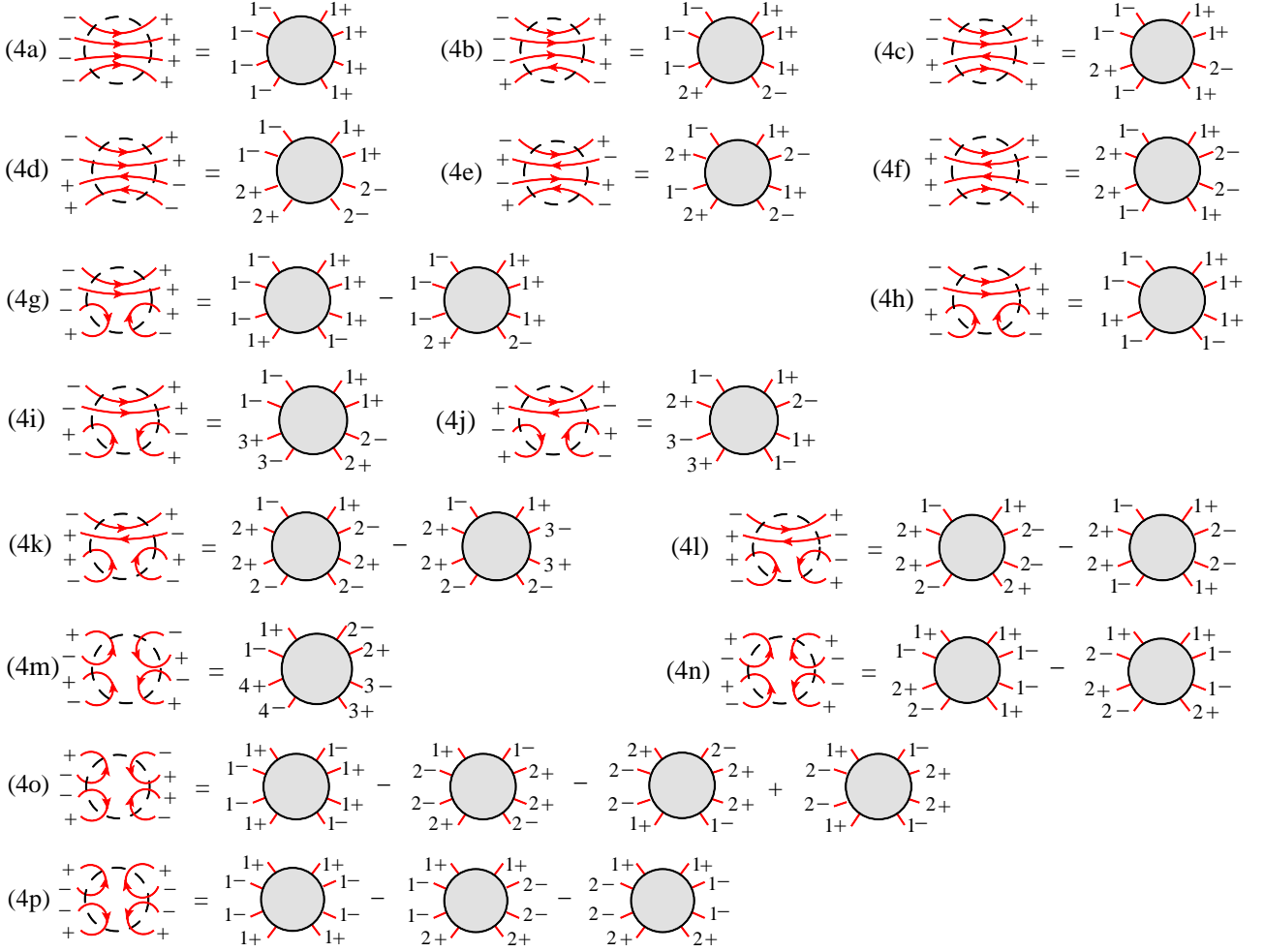


Figure 5: The possible fermion-line configurations for amplitudes with four fermion lines.

different terms, analogous to case (3e). Case (4p) requires three terms to remove all identical fermions; and case (4o) requires four separate terms. Case (4o) can be written as

$$\begin{aligned}
A^{\text{QCD}}(\bar{q}_1^-, q_1^+, \bar{q}_2^-, q_2^+, q_3^+, \bar{q}_3^-, q_4^+, \bar{q}_4^-) &= A^{\mathcal{N}=4 \text{ SYM}}(1^-, 1^+, 1^-, 1^+, 1^+, 1^-, 1^+, 1^-) \\
&- [A^{\mathcal{N}=4 \text{ SYM}}(2^-, 1^+, 1^-, 2^+, 2^+, 2^-, 2^+, 2^-) - A^{\mathcal{N}=4 \text{ SYM}}(2^-, 1^+, 1^-, 2^+, 2^+, 1^-, 1^+, 2^-)] \\
&- [A^{\mathcal{N}=4 \text{ SYM}}(2^-, 2^+, 2^-, 2^+, 2^+, 1^-, 1^+, 2^-) - A^{\mathcal{N}=4 \text{ SYM}}(2^-, 1^+, 1^-, 2^+, 2^+, 1^-, 1^+, 2^-)] \\
&- A^{\mathcal{N}=4 \text{ SYM}}(2^-, 1^+, 1^-, 2^+, 2^+, 1^-, 1^+, 2^-) \tag{3.2}
\end{aligned}$$

$$\begin{aligned}
&= A^{\mathcal{N}=4 \text{ SYM}}(1^-, 1^+, 1^-, 1^+, 1^+, 1^-, 1^+, 1^-) - A^{\mathcal{N}=4 \text{ SYM}}(2^-, 1^+, 1^-, 2^+, 2^+, 2^-, 2^+, 2^-) \\
&- A^{\mathcal{N}=4 \text{ SYM}}(2^-, 2^+, 2^-, 2^+, 2^+, 1^-, 1^+, 2^-) + A^{\mathcal{N}=4 \text{ SYM}}(2^-, 1^+, 1^-, 2^+, 2^+, 1^-, 1^+, 2^-). \tag{3.3}
\end{aligned}$$

The first form of this equation indicates that three different wrong-fermion-line configurations

have to be removed. However, all removals can be accomplished with the help of different permutations of two other cases, (4f) and (4l) respectively,

$$A^{\text{QCD}}(\bar{q}_1, q_1^+, \bar{q}_2, \bar{q}_3, q_4^+, \bar{q}_4, q_3^+, q_2^+) = A^{\mathcal{N}=4 \text{ SYM}}(1^-, 1^+, 2^-, 2^-, 1^+, 1^-, 2^+, 2^+), \quad (3.4)$$

$$\begin{aligned} & A^{\text{QCD}}(\bar{q}_1, q_1^+, \bar{q}_2, \bar{q}_3, q_3^+, \bar{q}_4, q_4^+, q_2^+) \\ &= A^{\mathcal{N}=4 \text{ SYM}}(1^-, 1^+, 2^-, 2^-, 2^+, 2^-, 2^+, 2^+) - A^{\mathcal{N}=4 \text{ SYM}}(1^-, 1^+, 2^-, 2^-, 1^+, 1^-, 2^+, 2^+). \end{aligned} \quad (3.5)$$

Case (4l) itself requires a wrong-fermion-line subtraction.

We have not yet ascertained whether any QCD tree amplitudes with more than four fermion lines are impossible to extract from $\mathcal{N} = 4$ super Yang-Mills theory. Fortunately, for a fixed number of external partons, as one increases the number of fermion lines the number of Feynman diagrams decreases. Also, amplitudes with many external quarks typically contribute much less to a multi-jet cross section than do amplitudes with more gluons and fewer quarks.

Finally, we remark on the conversion of pure-QCD tree amplitudes, that is amplitudes for quarks and gluons, into amplitudes that contain in addition a single electroweak vector boson, namely a W , Z or virtual photon. It is sufficient to compute the amplitude including the decay of the boson to a fermion-anti-fermion pair.

Consider first the case of a virtual photon which is emitted from a quark q and decays to a charged lepton (Drell-Yan) pair $\ell^+\ell^-$. We can extract this amplitude from a color-ordered amplitude with four consecutive fermions, as follows:

$$A^{\gamma^*}(\dots, q^+, \ell^-, \ell^+, \bar{q}^-, \dots) = A^{\text{QCD}}(\dots, q_1^+, \bar{q}_2^-, q_2^+, \bar{q}_1^-, \dots). \quad (3.6)$$

The color-ordering prevents gluons from being emitted from the quark line q_2 , or from the virtual gluon connecting q_1 and q_2 . Hence this virtual gluon is functionally identical to a virtual photon. The only other modification comes when dressing A^{γ^*} with couplings. There is a relative factor of $2(-Q^q)e^2/g^2$ when doing so, where the “2” is related to the standard normalizations of the QED interaction with coupling e , versus the QCD interaction with coupling g , and Q^q is the electric charge of the quark q . (The lepton has charge -1 .)

It is possible to extract the amplitude (3.6) a second way, using one quark flavor instead of two,

$$A^{\gamma^*}(\dots, q^+, \ell^-, \ell^+, \bar{q}^-, \dots) = -A^{\text{QCD}}(\dots, q_1^+, q_1^+, \bar{q}_1^-, \bar{q}_1^-, \dots). \quad (3.7)$$

This alternative works because the color-ordered interaction for $g^* \rightarrow q^+\bar{q}^-$ is antisymmetric under exchange of q and \bar{q} , and because the exchange of a gluon between identical-flavor quarks in the wrong channel is prevented by helicity conservation.

If the virtual photon decays to other charged massless fermions, *i.e.* to a quark-anti-quark pair $q'\bar{q}'$, the only difference is of course to use the appropriate quark charge, $-Q^qe^2 \rightarrow Q^qQ^{q'}e^2$. Because helicity amplitudes are used, it is also trivial to convert the virtual-photon amplitudes to ones for (parity-violating) electroweak boson production. For the case of combined exchange of virtual photon and Z boson, with decay to a charged lepton pair, the electric charge factor has to be replaced by

$$2e^2 \left(-Q^q + v_{L,R}^\ell v_{L,R}^q \mathcal{P}_Z(s_{\ell\bar{\ell}}) \right), \quad (3.8)$$

where $v_{L,R}^\ell$ are the left- and right-handed couplings of the lepton to the Z boson, $v_{L,R}^q$ are the corresponding quantities for the quark,

$$\mathcal{P}_Z(s) = \frac{s}{s - M_Z^2 + i \Gamma_Z M_Z} \quad (3.9)$$

is the ratio of Z to γ^* propagators, and M_Z and Γ_Z are the mass and width of the Z .

Whether v_L or v_R is to be used in eq. (3.8) depends on the helicity assignment, *i.e.* on whether the Z couples to a left- or right-handed outgoing fermion (as opposed to anti-fermion); see ref. [37] for further details. The case of a W^\pm boson is even simpler, because there is no coupling to right-handed fermions (and no interference with another boson).

The relevant MHV and NMHV amplitudes for four external fermions and the rest gluons, and for six external fermions and the rest gluons, have been converted in the above manner into tree amplitudes for $Vq\bar{q}g\dots g$ and $Vq\bar{q}Q\bar{Q}g\dots g$, where V stands for W , Z or γ^* . These NMHV amplitudes have been incorporated into the BLACKHAT library [31] and used there in conjunction with a numerical implementation [38] of the BCFW (on-shell) recursion relations [17] in order to obtain amplitudes at the NNMHV level and beyond. Including the MHV and NMHV formulae speeds up the numerical recursive algorithm by a factor of about four, in the present implementation. This approach was used to compute the real-radiative corrections entering the recent evaluation of $pp \rightarrow W + 4$ jets at NLO [27], in particular the tree amplitudes for $Wq\bar{q}'ggggg$ and $Wq\bar{q}'Q\bar{Q}ggg$. These amplitudes have nine external legs, after decaying the W boson to a lepton pair, so there are MHV, NMHV and NNMHV configurations, but no further. All seven-point configurations are either MHV or NMHV, so at most two recursive steps were required to hit an explicit formula (for example, in a schematic notation $A_9 \rightarrow A_8 \times A_3 \rightarrow A_7 \times A_3 \times A_3$).

We remark that the tree-level color-ordered amplitudes entering subleading-color loop amplitudes can have a more general color ordering from that required for purely tree-level applications. For example, in the pure QCD amplitudes with a single $q\bar{q}$ pair, only the color-ordered amplitudes in which the two fermions are adjacent are needed in eq. (3.1). However, the subleading-color terms in the one-loop amplitudes for $q\bar{q}g\dots g$ include many cases in which the two fermions are not color-adjacent, and the tree-level $q\bar{q}g\dots g$ amplitudes that enter their unitarity cuts have the same property. These color-ordered amplitudes are all available in $\mathcal{N} = 4$ super Yang-Mills theory, of course.

Similarly, for computing subleading-color one-loop terms for single-vector boson production processes like $Vq\bar{q}g\dots g$, one needs tree amplitudes such as $A^{\gamma^*}(\dots, q^+, g, \ell^-, \ell^+, \bar{q}^-, \dots)$, in which the gluon g is color-ordered with respect to the quark pair, but not the lepton pair. These amplitudes are not equal to any particular color-ordered amplitude in $\mathcal{N} = 4$ SYM, but one can generate them by summing over appropriate color orderings. For example, we have

$$\begin{aligned} A^{\gamma^*}(\dots, q^+, g, \ell^-, \ell^+, \bar{q}^-, \dots) &= A^{\text{QCD}}(\dots, q_1^+, g, \bar{q}_2^-, q_2^+, \bar{q}_1^-, \dots) \\ &+ A^{\text{QCD}}(\dots, q_1^+, \bar{q}_2^-, g, q_2^+, \bar{q}_1^-, \dots) + A^{\text{QCD}}(\dots, q_1^+, \bar{q}_2^-, q_2^+, g, \bar{q}_1^-, \dots). \end{aligned} \quad (3.10)$$

The sum over the three permutations properly cancels out the unwanted poles as g becomes collinear with either ℓ^- or ℓ^+ .

4 All gluon tree amplitudes

In this section we present the general expression for an n -gluon tree amplitude, which we derive in section 7 from the solution of ref. [21] for a general $\mathcal{N} = 4$ SYM super-amplitude.

Amplitudes for n -gluon scattering are classified by the number of negative-helicity gluons occurring in them. Tree-amplitudes with fewer than two negative-helicity gluons vanish. In our conventions the gluon at position n is always of negative helicity, which does not present a restriction due to cyclicity of the color-ordered amplitude. The Parke-Taylor formula [11] for a maximally-helicity-violating (MHV) gluon amplitude, with the two negative-helicity gluons sitting at positions $c_0 \in [1, n-1]$ and n , then reads

$$A_n(1^+, \dots, (c_0-1)^+, c_0^-, (c_0+1)^+, \dots, (n-1)^+, n^-) := A_n^{\text{MHV}}(c_0, n) = \frac{\delta^{(4)}(p) \langle c_0 n \rangle^4}{\langle 1 2 \rangle \langle 2 3 \rangle \dots \langle n 1 \rangle}, \quad (4.1)$$

with the total conserved momentum $p = \sum_{i=1}^n p_i$.

Next-to-maximally-helicity-violating amplitudes of degree p (N^pMHV) then consist of $(p+2)$ negative-helicity gluons embedded in $(n-p-2)$ positive-helicity states. We parametrize the positions of the negative-helicity gluons in the ordered set $(c_0, c_1, \dots, c_p, n)$ with $c_i \in [1, n-1]$.

The general N^pMHV tree-amplitude then takes the form

$$\boxed{A_n^{\text{N}^p\text{MHV}}(c_0, c_1, \dots, c_p, n) = \frac{\delta^{(4)}(p)}{\langle 12 \rangle \langle 23 \rangle \dots \langle n1 \rangle} \times \sum_{\text{all paths of length } p} 1 \cdot \tilde{R}_{n; a_1 b_1} \cdot \tilde{R}_{n; \{I_2\}; a_2 b_2}^{\{L_2\}; \{U_2\}} \cdot \dots \cdot \tilde{R}_{n; \{I_p\}; a_p b_p}^{\{L_p\}; \{U_p\}} \cdot \left(\det \Xi_n^{\text{path}}(c_0, \dots, c_p) \right)^4} \quad (4.2)$$

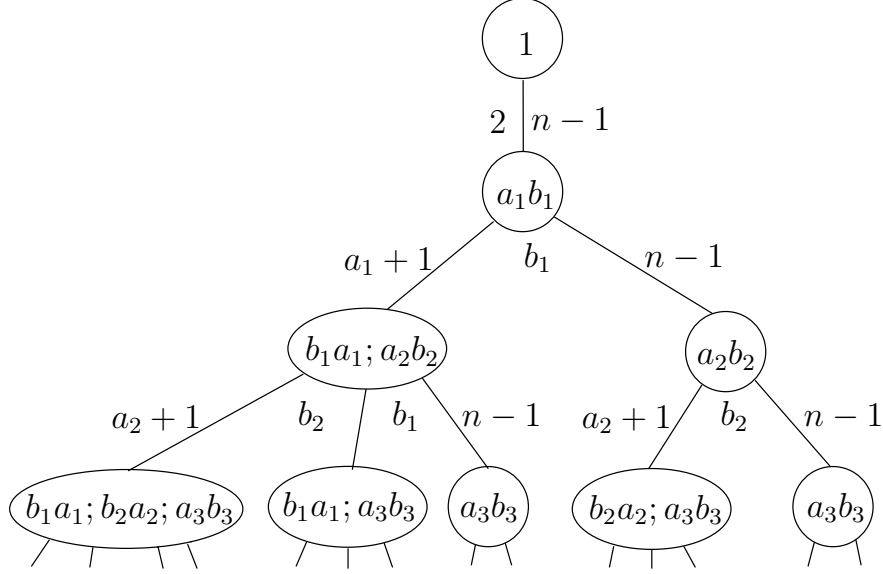
Let us now explain in turn the ingredients of this result, *i.e.* the sum over paths, the \tilde{R} -functions, and the path-matrix Ξ_n^{path} .

The sum over all paths refers to the rooted tree depicted in figure 6, introduced in ref. [21]. A path of length 0 consists of the initial node “1”. A path of length p leads to a sequence of $p+1$ nodes visited starting with node “1”. To clarify this all possible paths up to length $p=3$ are listed in figure 6. In general there are $(2p)!/(p!(p+1)!)$ different paths of length p , which is equal to the number of nodes appearing at level p in the rooted tree, since each final node unambiguously determines a path through the rooted tree.

The \tilde{R} -functions are generalizations of eq. (2.8) and may be written rather compactly with the help of eq. (2.6) as

$$\tilde{R}_{n; \{I\}; ab} := \frac{1}{x_{ab}^2} \frac{\langle a(a-1) \rangle}{\langle n \{I\} ba|a \rangle \langle n \{I\} ba|a-1 \rangle} \frac{\langle b(b-1) \rangle}{\langle n \{I\} ab|b \rangle \langle n \{I\} ab|b-1 \rangle}; \quad (4.3)$$

they derive from the dual superconformal R -invariants introduced in ref. [21]. In the above and in eq. (4.2), $\{I\}$ is a multi-index deriving from the node in the associated path with the last pair of indices stripped off, *e.g.* $\{I_3\} = \{b_1, a_1, b_2, a_2\}$ for the last node of the first path of length $p=3$.



Length p	Paths
0	[1]
1	[1] · [a ₁ , b ₁]
2	[1] · [a ₁ , b ₁] · [b ₁ , a ₁ ; a ₂ , b ₂] [1] · [a ₁ , b ₁] · [a ₂ , b ₂]
3	[1] · [a ₁ , b ₁] · [b ₁ , a ₁ ; a ₂ , b ₂] · [b ₁ , a ₁ , b ₂ , a ₂ ; a ₃ , b ₃] [1] · [a ₁ , b ₁] · [b ₁ , a ₁ ; a ₂ , b ₂] · [b ₁ , a ₁ ; a ₃ , b ₃] [1] · [a ₁ , b ₁] · [b ₁ , a ₁ ; a ₂ , b ₂] · [a ₃ , b ₃] [1] · [a ₁ , b ₁] · [a ₂ , b ₂] · [b ₂ , a ₂ ; a ₃ , b ₃] [1] · [a ₁ , b ₁] · [a ₂ , b ₂] · [a ₃ , b ₃]

Figure 6: The rooted tree encoding the sum over paths occurring in eq. (4.2). The table shows all paths up to length 3.

In eq. (4.2) we used a further piece of notation, namely \tilde{R} -functions with upper indices, which start to appear at the NNMHV level, and which we now define. Generally the \tilde{R} -functions appear in the amplitude with an ordered summation over the last pair of indices,

$$\sum_{L \leq a < b \leq U} \tilde{R}_{n; \{I\}; ab} . \quad (4.4)$$

\tilde{R} -functions with upper indices indicate a special behavior for the boundary terms in this sum when $a = L$ or $b = U$. Specifically if one has

$$\sum_{L \leq a < b \leq U} \tilde{R}_{n; \{I\}; ab}^{l_1, \dots, l_p; u_1, \dots, u_q} , \quad (4.5)$$

and the boundary of a summation is reached, then the occurrence of the spinor $|a-1\rangle$ or $|b\rangle$ in the \tilde{R} -function without upper indices (4.3) is replaced by a novel spinor depending on the upper indices as follows

$$\begin{aligned} \langle L-1| &\longrightarrow \langle \xi_L| := \langle n|x_{nl_1}x_{l_1l_2}\dots x_{l_{p-1}l_p} && \text{for } a = L, \\ \langle U| &\longrightarrow \langle \xi_U| := \langle n|x_{nu_1}x_{u_1u_2}\dots x_{u_{q-1}u_q} && \text{for } b = U. \end{aligned} \quad (4.6)$$

Effectively this amounts to the following formula for the upper-indexed \tilde{R} -functions of eq. (4.5),

$$\tilde{R}_{n;\{I\};ab}^{l_1,\dots,l_p;u_1,\dots,u_q} = \begin{cases} \tilde{R}_{n;\{I\};ab} \cdot \frac{\langle a\xi_L\rangle}{\langle n\{I\}ba|\xi_L\rangle} \frac{\langle n\{I\}ba|a-1\rangle}{\langle a(a-1)\rangle} & \text{for } a = L, \\ \tilde{R}_{n;\{I\};ab} \cdot \frac{\langle \xi_U(b-1)\rangle}{\langle n\{I\}ab|\xi_U\rangle} \frac{\langle n\{I\}ab|b\rangle}{\langle b(b-1)\rangle} & \text{for } b = U, \\ \tilde{R}_{n;\{I\};ab} \cdot \frac{\langle a\xi_L\rangle}{\langle n\{I\}ba|\xi_L\rangle} \frac{\langle n\{I\}ba|a-1\rangle}{\langle a(a-1)\rangle} \frac{\langle \xi_U(b-1)\rangle}{\langle n\{I\}ab|\xi_U\rangle} \frac{\langle n\{I\}ab|b\rangle}{\langle b(b-1)\rangle} & \text{for } a = L \text{ and } b = U, \\ \tilde{R}_{n;\{I\};ab} & \text{else.} \end{cases} \quad (4.7)$$

In particular there is a term in the double sum where both $a = L$ and $b = U$ are reached and both replacements are to be made. The rules for constructing the sets of upper indices $l_1, \dots, l_p; u_1, \dots, u_q$ in eq. (4.5) from the rooted tree are given in ref. [21].

To write down the path-matrix Ξ_n^{path} we furthermore need to define the quantities

$$(\Xi_n)_0^{c_i} := \langle nc_i \rangle, \quad (4.8)$$

$$(\Xi_n)_{ab}^{c_i} := \langle nba|c_i\rangle \chi_{[a,b-1]}(c_i) - x_{ab}^2 \langle nc_i\rangle \chi_{[b,n-1]}(c_i), \quad (4.9)$$

$$(\Xi_n)_{\{b_1,a_1,\dots,b_r,a_r\};ab}^{c_i} := \langle nb_1a_1\dots b_r a_r ab|c_i\rangle \chi_{[a,b-1]}(c_i) - x_{ab}^2 \langle nb_1a_1\dots b_r a_r |c_i\rangle \chi_{[a_r,a-1]}(c_i), \quad (4.10)$$

with the support functions

$$\chi_{[a,b]}(i) = \begin{cases} 1 & \text{if } i \in [a, b], \\ 0 & \text{else.} \end{cases} \quad (4.11)$$

Now to every node $[\{I\}; ab]$ along a given path and to every negative-helicity leg c_i we associate the entry of the path-matrix $(\Xi_n)_{\{I\};ab}^{c_i}$. The entries $(\Xi_n)^A_B$ form a $(p+1) \times (p+1)$ matrix. Explicitly one has

$$\Xi_n^{\text{path}}(c_0, \dots, c_p) := \begin{pmatrix} \langle nc_0\rangle & \langle nc_1\rangle & \dots & \langle nc_p\rangle \\ (\Xi_n)_{a_1b_1}^{c_0} & (\Xi_n)_{a_1b_1}^{c_1} & \dots & (\Xi_n)_{a_1b_1}^{c_p} \\ (\Xi_n)_{\{I_2\};a_2b_2}^{c_0} & (\Xi_n)_{\{I_2\};a_2b_2}^{c_1} & \dots & (\Xi_n)_{\{I_2\};a_2b_2}^{c_p} \\ \vdots & \vdots & & \vdots \\ (\Xi_n)_{\{I_p\};a_p b_p}^{c_0} & (\Xi_n)_{\{I_p\};a_p b_p}^{c_1} & \dots & (\Xi_n)_{\{I_p\};a_p b_p}^{c_p} \end{pmatrix}. \quad (4.12)$$

Although \tilde{R} and Ξ_n^{path} look rather involved at first sight, they are determined entirely through the external spinors λ_i and $\tilde{\lambda}_i$.

To clarify the construction principle let us write down the first three amplitudes in the N^p MHV series explicitly:

$$A_n^{\text{MHV}}(c_0, n) = \frac{\delta^{(4)}(p)}{\langle 12 \rangle \langle 23 \rangle \dots \langle n1 \rangle} \cdot \langle nc_0 \rangle^4, \quad (4.13)$$

$$A_n^{\text{NMHV}}(c_0, c_1, n) = \frac{\delta^{(4)}(p)}{\langle 12 \rangle \langle 23 \rangle \dots \langle n1 \rangle} \sum_{2 \leq a_1 < b_1 \leq n-1} \tilde{R}_{n;a_1 b_1} \cdot \left| \begin{array}{cc} \langle nc_0 \rangle & \langle nc_1 \rangle \\ (\Xi_n)_{a_1 b_1}^{c_0} & (\Xi_n)_{a_1 b_1}^{c_1} \end{array} \right|^4, \quad (4.14)$$

$$A_n^{\text{N}^2\text{MHV}}(c_0, c_1, c_2, n) = \frac{\delta^{(4)}(p)}{\langle 12 \rangle \langle 23 \rangle \dots \langle n1 \rangle} \sum_{2 \leq a_1 < b_1 < n} \tilde{R}_{n;a_1 b_1} \cdot \left[\begin{array}{c} \sum_{a_1+1 \leq a_2 < b_2 \leq b_1} \tilde{R}_{n;b_1 a_1; a_2 b_2}^{0;a_1 b_1} \cdot \left| \begin{array}{ccc} \langle nc_0 \rangle & \langle nc_1 \rangle & \langle nc_2 \rangle \\ (\Xi_n)_{a_1 b_1}^{c_0} & (\Xi_n)_{a_1 b_1}^{c_1} & (\Xi_n)_{a_1 b_1}^{c_2} \\ (\Xi_n)_{b_1, a_1; a_2 b_2}^{c_0} & (\Xi_n)_{b_1, a_1; a_2 b_2}^{c_1} & (\Xi_n)_{b_1, a_1; a_2 b_2}^{c_2} \end{array} \right|^4 \\ + \sum_{b_1 \leq a_2, b_2 < n} \tilde{R}_{n;a_2 b_2}^{a_1 b_1; 0} \cdot \left| \begin{array}{ccc} \langle nc_0 \rangle & \langle nc_1 \rangle & \langle nc_2 \rangle \\ (\Xi_n)_{a_1 b_1}^{c_0} & (\Xi_n)_{a_1 b_1}^{c_1} & (\Xi_n)_{a_1 b_1}^{c_2} \\ (\Xi_n)_{a_2 b_2}^{c_0} & (\Xi_n)_{a_2 b_2}^{c_1} & (\Xi_n)_{a_2 b_2}^{c_2} \end{array} \right|^4 \end{array} \right]. \quad (4.15)$$

In appendix A we spell out the NMHV and N^2 MHV amplitudes explicitly. We provide a `Mathematica` package `GGT` with the [arXiv.org](https://arxiv.org) submission of this article, which expands the master formula (4.2) explicitly for any choice of p , positions c_i and momenta $\lambda_i, \tilde{\lambda}_i$. See appendix C for documentation. The formula (4.2) is implemented by the function `GGTgluon`.

It should be mentioned that in practice the number of terms arising from the determinants of the path-matrix Ξ_n^{path} is often quite small, see *e.g.* eq. (2.7). Moreover, for small n the number of non-zero terms in the nested sums can be relatively small.

5 All single-flavor quark-anti-quark-gluon trees

Turning to the gauge-theory amplitudes involving massless single-flavor quark-anti-quark pairs we can write down a similarly general formula based on paths along the rooted tree of figure 6. In an abuse of notation, we refer here to a helicity $+\frac{1}{2}$ fermion as a quark, and a helicity $-\frac{1}{2}$ fermion as an anti-quark. Looking at a color-ordered n -parton amplitude involving gluons and k quark-anti-quark pairs, $g^{n-2k}(q\bar{q})^k$, it is again classified as a N^p MHV amplitude by the number $(2+p-k)$ of negative-helicity gluons. In such a color-ordered amplitude we furthermore consider an arbitrary ordering of the fermions. We then have $2+p+k$ ‘special’ legs (negative-helicity gluon, quark or anti-quark) in such an amplitude, whose position amongst the n legs we parametrize by the set

$$(c_0, \dots, c_{\alpha_1}, \dots, c_{\bar{\beta}_1}, \dots, c_{\alpha_k}, \dots, c_{\bar{\beta}_k}, \dots, c_{p+k}, n). \quad (5.1)$$

Here c_i denotes the position of a negative-helicity gluon, c_{α_j} a quark and $c_{\bar{\beta}_j}$ an anti-quark location. Note that while the quark and anti-quark locations c_{α_i} and $c_{\bar{\beta}_i}$ are considered as ordered sets, *i.e.* $c_{\alpha_i} < c_{\alpha_j}$ and $c_{\bar{\beta}_i} < c_{\bar{\beta}_j}$ for $i < j$, there is no such ordering in the total set $\{c_{\alpha_i}, c_{\bar{\beta}_i}\}$

reflecting an arbitrary sequence of quarks and anti-quarks in the color-ordered amplitude. Again in our convention one negative-helicity gluon is always located on leg n^1 .

The general N^pMHV tree-amplitude for such a configuration then reads

$$A_{(q\bar{q})^k, n}^{\text{N}^p\text{MHV}}(c_0, \dots, c_{\alpha_1}, \dots, c_{\bar{\beta}_1}, \dots, c_{\alpha_k}, \dots, c_{\bar{\beta}_k}, \dots, c_{p+k}, n) = \frac{\delta^{(4)}(p)}{\langle 1 2 \rangle \langle 2 3 \rangle \dots \langle n 1 \rangle} \times \text{sign}(\tau) \sum_{\substack{\text{all paths} \\ \text{of length } p}} \left(\prod_{i=1}^p \tilde{R}_{n; \{I_i\}; a_i b_i}^{\{L_i\}; \{U_i\}} \right) \det \left(\Xi_n^{\text{path}} \Big|_q \right)^3 \det \left(\Xi_n^{\text{path}}(\bar{q} \leftrightarrow q) \Big|_{\bar{q}} \right). \quad (5.2)$$

Here $\text{sign}(\tau)$ is the sign produced by permuting the quark and anti-quark legs into the alternating order $\{c_{\alpha_1}, c_{\bar{\beta}_1}, c_{\alpha_2}, c_{\bar{\beta}_2}, \dots, c_{\alpha_k}, c_{\bar{\beta}_k}\}$.

Remarkably, the only difference from the pure gluon amplitudes is a change in the determinant factors of the path-matrix Ξ_n^{path} . With $2 + p + k$ ‘special’ legs the path-matrix associated to eq. (5.1) is now a $(p + 1) \times (p + 1 + k)$ matrix of the form

$$\Xi_n^{\text{path}} := \begin{pmatrix} \langle nc_0 \rangle & \dots & \langle nc_{\alpha_i} \rangle & \dots & \langle nc_{\bar{\beta}_i} \rangle & \dots & \langle nc_{p+k} \rangle \\ (\Xi_n)_{a_1 b_1}^{c_0} & \dots & (\Xi_n)_{a_1 b_1}^{c_{\alpha_i}} & \dots & (\Xi_n)_{a_1 b_1}^{c_{\bar{\beta}_i}} & \dots & (\Xi_n)_{a_1 b_1}^{c_p} \\ (\Xi_n)_{\{I_2\}; a_2 b_2}^{c_0} & \dots & (\Xi_n)_{\{I_2\}; a_2 b_2}^{c_{\alpha_i}} & \dots & (\Xi_n)_{\{I_2\}; a_2 b_2}^{c_{\bar{\beta}_i}} & \dots & (\Xi_n)_{\{I_2\}; a_2 b_2}^{c_p} \\ \vdots & & \vdots & & \vdots & & \vdots \\ (\Xi_n)_{\{I_p\}; a_p b_p}^{c_0} & \dots & (\Xi_n)_{\{I_p\}; a_p b_p}^{c_{\alpha_i}} & \dots & (\Xi_n)_{\{I_p\}; a_p b_p}^{c_{\bar{\beta}_i}} & \dots & (\Xi_n)_{\{I_p\}; a_p b_p}^{c_p} \end{pmatrix} \quad (5.3)$$

The notation $\Xi_n^{\text{path}} \Big|_q$ in eq. (5.2) now refers to the elimination of all the quark columns (the c_{α_i} ’s) in the path-matrix and $\Xi_n^{\text{path}}(\bar{q} \leftrightarrow q) \Big|_{\bar{q}}$ denotes the matrix with all the anti-quark columns removed (the $c_{\bar{\beta}_i}$ ’s) after quark and anti-quark columns have been interchanged, *i.e.* $c_{\bar{\beta}_i} \leftrightarrow c_{\alpha_i}$. The removal of k columns is of course necessary in order to turn the $(p + 1 + k) \times (p + 1)$ matrix Ξ_n^{path} into square form, so that the determinant is defined.

Let us again spell out some of the lower p amplitudes explicitly to clarify the formula (5.2):

$$A_{q\bar{q}, n}^{\text{MHV}}(c_{\alpha_1}, c_{\bar{\beta}_1}, n) = \frac{\delta^{(4)}(p)}{\langle 12 \rangle \langle 23 \rangle \dots \langle n1 \rangle} \cdot \langle nc_{\bar{\beta}_1} \rangle^3 \cdot \langle nc_{\alpha_1} \rangle \quad (5.4)$$

$$A_{q\bar{q}, n}^{\text{NMHV}}(c_0, c_{\alpha_1}, c_{\bar{\beta}_1}, n) = \frac{\delta^{(4)}(p)}{\langle 12 \rangle \langle 23 \rangle \dots \langle n1 \rangle} \sum_{2 \leq a_1 < b_1 \leq n-1} \tilde{R}_{n; a_1 b_1} \cdot \begin{vmatrix} \langle nc_0 \rangle & \langle nc_{\bar{\beta}_1} \rangle \\ (\Xi_n)_{a_1 b_1}^{c_0} & (\Xi_n)_{a_1 b_1}^{c_{\bar{\beta}_1}} \end{vmatrix}^3 \cdot \begin{vmatrix} \langle nc_0 \rangle & \langle nc_{\alpha_1} \rangle \\ (\Xi_n)_{a_1 b_1}^{c_0} & (\Xi_n)_{a_1 b_1}^{c_{\alpha_1}} \end{vmatrix} \quad (5.5)$$

$$A_{(q\bar{q})^2, n}^{\text{NMHV}}(c_{\alpha_1}, c_{\bar{\beta}_1}, c_{\alpha_2}, c_{\bar{\beta}_2}, n) = \frac{\delta^{(4)}(p)}{\langle 12 \rangle \langle 23 \rangle \dots \langle n1 \rangle} \sum_{2 \leq a_1 < b_1 \leq n-1} \tilde{R}_{n; a_1 b_1}.$$

¹We comment in section 7 on how to circumvent this problem for the case without a single negative-helicity gluon.

$$\begin{aligned}
& \left| \begin{array}{cc} \langle nc_{\bar{\beta}_1} \rangle & \langle nc_{\bar{\beta}_2} \rangle \\ (\Xi_n)_{a_1 b_1}^{c_{\bar{\beta}_1}} & (\Xi_n)_{a_1 b_1}^{c_{\bar{\beta}_2}} \end{array} \right|^3 \cdot \left| \begin{array}{cc} \langle nc_{\alpha_1} \rangle & \langle nc_{\alpha_2} \rangle \\ (\Xi_n)_{a_1 b_1}^{c_{\alpha_1}} & (\Xi_n)_{a_1 b_1}^{c_{\alpha_2}} \end{array} \right| \quad (5.6) \\
A_{q\bar{q},n}^{\text{N}^2\text{MHV}}(c_{\alpha_1}, c_1, c_{\bar{\beta}_1}, c_2, n) &= \frac{\delta^{(4)}(p)}{\langle 12 \rangle \langle 23 \rangle \dots \langle n1 \rangle} \sum_{2 \leq a_1 < b_1 < n} \tilde{R}_{n;a_1 b_1} \cdot \\
& \left[\sum_{a_1+1 \leq a_2 < b_2 \leq b_1} \tilde{R}_{n;b_1 a_1; a_2 b_2}^{0; a_1 b_1} \cdot \left| \begin{array}{ccc} \langle nc_1 \rangle & \langle nc_{\bar{\beta}_1} \rangle & \langle nc_2 \rangle \\ (\Xi_n)_{a_1 b_1}^{c_1} & (\Xi_n)_{a_1 b_1}^{c_{\bar{\beta}_1}} & (\Xi_n)_{a_1 b_1}^{c_2} \\ (\Xi_n)_{b_1, a_1; a_2 b_2}^{c_1} & (\Xi_n)_{b_1, a_1; a_2 b_2}^{c_{\bar{\beta}_1}} & (\Xi_n)_{b_1, a_1; a_2 b_2}^{c_2} \end{array} \right|^3 \cdot \right. \\
& \left. + \sum_{b_1 \leq a_2, b_2 < n} \tilde{R}_{n;a_2 b_2}^{a_1 b_1; 0} \cdot \left| \begin{array}{ccc} \langle nc_1 \rangle & \langle nc_{\bar{\beta}_1} \rangle & \langle nc_2 \rangle \\ (\Xi_n)_{a_1 b_1}^{c_1} & (\Xi_n)_{a_1 b_1}^{c_{\bar{\beta}_1}} & (\Xi_n)_{a_1 b_1}^{c_2} \\ (\Xi_n)_{a_2 b_2}^{c_1} & (\Xi_n)_{a_2 b_2}^{c_{\bar{\beta}_1}} & (\Xi_n)_{a_2 b_2}^{c_2} \end{array} \right|^3 \left| \begin{array}{ccc} \langle nc_1 \rangle & \langle nc_{\alpha_1} \rangle & \langle nc_2 \rangle \\ (\Xi_n)_{a_1 b_1}^{c_1} & (\Xi_n)_{a_1 b_1}^{c_{\alpha_1}} & (\Xi_n)_{a_1 b_1}^{c_2} \\ (\Xi_n)_{a_2 b_2}^{c_1} & (\Xi_n)_{a_2 b_2}^{c_{\alpha_1}} & (\Xi_n)_{a_2 b_2}^{c_2} \end{array} \right| \right] \quad (5.7)
\end{aligned}$$

$$\begin{aligned}
A_{(q\bar{q})^2, n}^{\text{N}^2\text{MHV}}(c_{\alpha_1}, c_1, c_{\bar{\beta}_1}, c_{\alpha_2}, c_{\bar{\beta}_2}, n) &= \frac{\delta^{(4)}(p)}{\langle 12 \rangle \langle 23 \rangle \dots \langle n1 \rangle} \sum_{2 \leq a_1 < b_1 < n} \tilde{R}_{n;a_1 b_1} \cdot \\
& \left[\sum_{a_1+1 \leq a_2 < b_2 \leq b_1} \tilde{R}_{n;b_1 a_1; a_2 b_2}^{0; a_1 b_1} \cdot \left| \begin{array}{ccc} \langle nc_1 \rangle & \langle nc_{\bar{\beta}_1} \rangle & \langle nc_{\bar{\beta}_2} \rangle \\ (\Xi_n)_{a_1 b_1}^{c_1} & (\Xi_n)_{a_1 b_1}^{c_{\bar{\beta}_1}} & (\Xi_n)_{a_1 b_1}^{c_{\bar{\beta}_2}} \\ (\Xi_n)_{b_1, a_1; a_2 b_2}^{c_1} & (\Xi_n)_{b_1, a_1; a_2 b_2}^{c_{\bar{\beta}_1}} & (\Xi_n)_{b_1, a_1; a_2 b_2}^{c_{\bar{\beta}_2}} \end{array} \right|^3 \cdot \right. \\
& \left. + \sum_{b_1 \leq a_2 < b_2 < n} \tilde{R}_{n;a_2 b_2}^{a_1 b_1; 0} \cdot \left| \begin{array}{ccc} \langle nc_1 \rangle & \langle nc_{\bar{\beta}_1} \rangle & \langle nc_{\bar{\beta}_2} \rangle \\ (\Xi_n)_{a_1 b_1}^{c_1} & (\Xi_n)_{a_1 b_1}^{c_{\bar{\beta}_1}} & (\Xi_n)_{a_1 b_1}^{c_{\bar{\beta}_2}} \\ (\Xi_n)_{a_2 b_2}^{c_1} & (\Xi_n)_{a_2 b_2}^{c_{\bar{\beta}_1}} & (\Xi_n)_{a_2 b_2}^{c_{\bar{\beta}_2}} \end{array} \right|^3 \left| \begin{array}{ccc} \langle nc_1 \rangle & \langle nc_{\alpha_1} \rangle & \langle nc_{\alpha_2} \rangle \\ (\Xi_n)_{a_1 b_1}^{c_1} & (\Xi_n)_{a_1 b_1}^{c_{\alpha_1}} & (\Xi_n)_{a_1 b_1}^{c_{\alpha_2}} \\ (\Xi_n)_{a_2 b_2}^{c_1} & (\Xi_n)_{a_2 b_2}^{c_{\alpha_1}} & (\Xi_n)_{a_2 b_2}^{c_{\alpha_2}} \end{array} \right| \right] \quad (5.8)
\end{aligned}$$

This completes our examples. Some explicit formulae with the determinants expanded out may be found in appendix B. The formula (5.2) is implemented in `GGT` by the function `GGTfermionS`. See appendix C for the documentation.

Note that the master formula (4.2) reduces as it should to the pure-gluon scattering result (4.2) for a zero number of quark-anti-quark pairs, $k \rightarrow 0$. In that case no column removals are to be performed and the determinants combine to the power four.

6 All gluon-gluino tree amplitudes in $\mathcal{N} = 4$ super Yang-Mills

The color-ordered tree amplitudes with fermions presented above were special in the sense that they apply both to massless QCD as well as $\mathcal{N} = 4$ super Yang-Mills, due to the single-flavor choice which suppresses intermediate scalar exchange as argued in section 3. We now state the master formula for general gluino and gluon tree amplitudes in the $\mathcal{N} = 4$ super Yang-Mills theory from which the above expressions arise. Through specific choices of external flavor configurations, however, this master formula may be used to produce color-ordered gluon and quark trees in massless QCD, as was discussed in section 3.

Similar to the notation in section 5, for a general $g^{n-2k}(q\bar{q})^k$ amplitude with arbitrary flavor assignments to the ‘quarks’² we have $2 + p + k$ ‘special’ legs (negative-helicity gluon, quark or anti-quark), whose position amongst the n legs we parametrize by the set

$$(c_0, \dots, c_{\alpha_1}^{A_1}, \dots, c_{\beta_1}^{B_1}, \dots, c_{\alpha_k}^{A_k}, \dots, c_{\beta_k}^{B_k}, \dots, c_{p+k}, n). \quad (6.1)$$

Again the configuration of quarks and anti-quarks inside the gluon background may be arbitrary while the sets $\{\alpha_i\}$ and $\{\beta_i\}$ are ordered. The general $g^{n-2k}(q\bar{q})^k$ amplitude with $(2 + p - k)$ negative-helicity gluons is then expressed in terms of the R -functions and the path-matrix $\Xi_{(q\bar{q})^k, n}^{\text{path}}$ defined above. It reads

$$\boxed{A_{(q\bar{q})^k, n}^{\text{NPMHV}}(c_0, \dots, c_{\alpha_i}^{A_i}, \dots, c_{\beta_j}^{B_j}, \dots, c_{p+k}, n) = \frac{\delta^{(4)}(p) \text{sign}(\tau)}{\langle 1 2 \rangle \langle 2 3 \rangle \dots \langle n 1 \rangle} \times} \\ \times \sum_{\substack{\text{all paths} \\ \text{of length } p}} \left(\prod_{i=1}^p \tilde{R}_{n; \{I_i\}; \{U_i\}} \right) \left(\det \Xi_n^{\text{path}} \Big|_q \right)^{4-k} \times \\ \times \sum_{\sigma \in S_k} \text{sign}(\sigma) \prod_{i=1}^k \delta^{A_i B_{\sigma(i)}} \det \left(\Xi_n^{\text{path}} \Big|_q (\bar{\beta}_{\sigma(i)} \leftrightarrow \alpha_i) \right). \quad (6.2)$$

Here the notation $\Xi_n^{\text{path}}|_q$ refers to the path-matrix (5.3) with all ‘quark’ columns $\{c_{\alpha_i}\}$ removed, whereas $\Xi_n^{\text{path}}|_q(\bar{\beta}_i \rightarrow \alpha_i)$ denotes the same path-matrix where the ‘anti-quark’ column c_{β_j} is replaced by one of the previously-removed ‘quark’ columns c_{α_i} . Also $\text{sign}(\tau)$ is the sign of the permutation for bringing the initial color-ordering of the fermionic legs into the canonical order $\{c_{\alpha_1}, c_{\beta_1}, c_{\alpha_2}, c_{\beta_2}, \dots, c_{\alpha_k}, c_{\beta_k}\}$ and $\text{sign}(\sigma)$ is the sign of the permutation of σ . This formula is implemented in `GGT` by the function `GGTfermion`.

7 Proof of the master formula

In this section we prove the master formula (6.2) for a general $\mathcal{N} = 4$ super Yang-Mills tree amplitude with external gluons and gluinos of arbitrary flavor, as well as the more compact

²We refer to the gluinos in this and the following sections as ‘quarks’ in order to not introduce new terminology beyond that introduced already in sections 4 and 5.

single-flavor expression (5.2) and the pure gluon expression (4.2) as sub-cases.

Amplitudes in $\mathcal{N} = 4$ super Yang-Mills are very efficiently expressed in terms of a superwave function Φ which collects all on-shell states of the PCT self-conjugate massless $\mathcal{N} = 4$ multiplet, with the help of the Grassmann variables η^A with $A = 1, 2, 3, 4$ of the $su(4)$ R-symmetry,

$$\begin{aligned} \Phi(\lambda, \tilde{\lambda}, \eta) = & g^+(\lambda, \tilde{\lambda}) + \eta^A \tilde{g}_A(\lambda, \tilde{\lambda}) + \frac{1}{2} \eta^A \eta^B \phi_{AB}(\lambda, \tilde{\lambda}) + \frac{1}{3!} \eta^A \eta^B \eta^C \epsilon_{ABCD} \bar{g}^D(\lambda, \tilde{\lambda}) \\ & + \frac{1}{4!} \eta^A \eta^B \eta^C \eta^D \epsilon_{ABCD} g^-(\lambda, \tilde{\lambda}). \end{aligned} \quad (7.1)$$

Here g^\pm are the ± 1 helicity gluons, \tilde{g}_A and \bar{g}^A the four flavor $\pm \frac{1}{2}$ helicity gluinos, and ϕ_{AB} the six real 0 helicity scalar states. The Grassmann variables η carry helicity $+\frac{1}{2}$ so that the whole multiplet carries helicity $+1$.

We can write the amplitudes in the on-shell superspace with coordinates $(\lambda_i, \tilde{\lambda}_i, \eta_i)$ [12, 16, 39],

$$\mathcal{A}_n(\lambda_i, \tilde{\lambda}_i, \eta_i) = \mathcal{A}(\Phi_1 \dots \Phi_n). \quad (7.2)$$

Since the helicity of each supermultiplet Φ_i is 1 the amplitude obeys

$$h_i \mathcal{A}_n(\lambda_i, \tilde{\lambda}_i, \eta_i) = \mathcal{A}_n(\lambda_i, \tilde{\lambda}_i, \eta_i), \quad (7.3)$$

where h_i is the helicity operator for the i th leg. The component field amplitudes are then obtained by projecting upon the relevant terms in the η_i expansion of the super-amplitude via

$$g_i^+ \rightarrow \eta_i^A = 0, \quad g_i^- \rightarrow \int d^4 \eta_i = \int d\eta_i^1 d\eta_i^2 d\eta_i^3 d\eta_i^4, \quad \tilde{g}_{i,A} \rightarrow \int d\eta^A, \quad \bar{g}_i^A \rightarrow - \int d^4 \eta_i \eta_i^A. \quad (7.4)$$

Note that the super-amplitude \mathcal{A}_n has a cyclic symmetry that can lead to many different but equivalent expressions in practice. In order to obtain compact expressions for component amplitudes often a judicious choice of this cyclic freedom can be made [21].

The general solution for tree super-amplitudes of Drummond and one of the present authors [21] takes the compact form

$$\mathcal{A}_n^{\text{N}^p\text{MHV}} = \frac{\delta^{(4)}(p) \delta^{(8)}(q)}{\langle 12 \rangle \langle 23 \rangle \dots \langle n1 \rangle} \sum_{\text{all paths of length } p} 1 \cdot R_{n,a_1 b_1} \cdot R_{n,\{I_2\},a_2 b_2} \cdot \dots \cdot R_{n,\{I_p\},a_p b_p}, \quad (7.5)$$

where $q^{\alpha A} = \sum_{i=1}^n \lambda_i^\alpha \eta_i^A$ is the total conserved fermionic momentum, and the dual superconformal R -invariant is

$$R_{n,\{I\},ab} = \tilde{R}_{n,\{I\},ab} \delta^{(4)} \left(\sum_{i=1}^n \Xi_{n,\{I\},ab}(i) \eta_i \right), \quad (7.6)$$

in the notation of the previous sections. We now wish to project this result in on-shell superspace onto the relevant components for a general $g^{n-2k}(q\bar{q})^k$ amplitude. For this purpose we set all of the η_i associated to positive-helicity gluon states to zero. This leaves us with the $p + 2 + k$ remaining Grassmann numbers η_{c_i} associated to the ‘special’ legs of helicities -1 and $\pm \frac{1}{2}$. To

project onto a negative-gluon state at position i one simply has to integrate eq. (7.5) against $\int d^4\eta_i$. Similarly, to project to a quark or anti-quark state at position i of flavor A_i one integrates eq. (7.5) against $\int d\eta_i^{A_i}$ or $-\int d^4\eta_i \eta_i^{A_i}$. All integrations have to be in color order.

In accord with our convention above the leg n is chosen to be a negative-helicity gluon state, or an anti-quark if there are no negative-helicity gluons. This is a convenient choice because the only dependence of the super-amplitude on η_n is through the total fermionic momentum conserving delta function, which can be written as

$$\delta^{(8)}(q) = \delta^{(8)}\left(\sum_{i=0}^{p+k} \lambda_{c_i} \eta_{c_i} + \lambda_n \eta_n\right) = \delta^{(4)}\left(\sum_{i=1}^{p+k} \frac{\langle c_0 c_i \rangle}{\langle c_0 n \rangle} \eta_{c_i} + \eta_n\right) \delta^{(4)}\left(\sum_{i=0}^{p+k} \langle n c_i \rangle \eta_{c_i}\right). \quad (7.7)$$

For each path in eq. (7.5) the four-dimensional Grassmann delta functions in eq. (7.7), together with the p delta functions arising from the R -invariants (7.6), may be written as

$$\prod_{i=0}^{p+1} \delta^{(4)}\left(\sum_{j=0}^{p+k} (\Xi_n^{\text{path}})_{ij} \eta_{c_j}\right) := \delta^{(4)}\left(\sum_{i=1}^{p+k} \frac{\langle c_0 c_i \rangle}{\langle c_0 n \rangle} \eta_{c_i} + \eta_n\right) \delta^{(4)}\left(\sum_{i=0}^{p+k} \langle n c_i \rangle \eta_{c_i}\right) \prod_{i=1}^p \delta^{(4)}\left(\sum_{j=0}^{p+k} \Xi_{n; \{I_i\}; a_i b_i}(c_j) \eta_{c_j}\right), \quad (7.8)$$

with the $(p+2) \times (p+k+2)$ path-matrix Ξ_n^{path} . If we have a negative-helicity gluon at position n , the η_n integration is trivial and we can drop the trial η_n column and the row determined by the first delta function in eq. (7.8), ending up with the $(p+1) \times (p+k+1)$ path-matrix given in eq. (5.3). For the sake of readability we will drop the labels on the path-matrix in what follows, just denoting it by Ξ , and assume a negative-helicity gluon at position n . The projection to the general $g^{n-2k}(q\bar{q})^k$ amplitude of eq. (4.2), with quarks of flavor A_i at positions c_{α_i} and anti-quarks of flavor B_j at positions $c_{\bar{\beta}_j}$,

$$A_{(q\bar{q})^k, n}^{\text{NPMHV}}(c_0, \dots, c_{\alpha_i}^{A_i}, \dots, c_{\bar{\beta}_j}^{B_j}, \dots, c_{p+k}, n),$$

is then performed via the Grassmann integrals

$$(-1)^k \text{sign}(\tau) \left(\prod_{\substack{j=0 \\ j \notin \{\alpha_1, \dots, \alpha_k\}}}^{p+k} \int d^4\eta_{c_j} \right) \left(\prod_{l=1}^k \int d\eta_{c_{\alpha_l}}^{A_l} \eta_{c_{\bar{\beta}_l}}^{B_l} \right) \prod_{i=0}^{p+1} \delta^{(4)}\left(\sum_{j=0}^{p+k} \Xi_{ij} \eta_{c_j}\right). \quad (7.9)$$

Here $\text{sign}(\tau)$ compensates the minus signs we encountered by permuting the quark and anti-quark Grassmann variables from color order to the canonical order $\prod_{l=1}^k \int d\eta_{c_{\alpha_l}}^{A_l} \eta_{c_{\bar{\beta}_l}}^{B_l}$.

Let us first consider the pure gluon case, *i.e.* $k = 0$. Performing the change of variables $\eta_{c_i} \rightarrow \Xi_{ij}^{-1} \eta_{c_j}$ immediately gives

$$\left(\prod_{j=0}^p \int d^4\eta_{c_j} \right) \prod_{i=0}^{p+1} \delta^{(4)}\left(\sum_{j=0}^p \Xi_{ij} \eta_{c_j}\right) = (\det \Xi)^4, \quad (7.10)$$

thereby proving eq. (4.2). To evaluate the general integral (7.9) we first perform the $(p+1)$ four-dimensional integrations with respect to the η 's of the anti-quarks and gluons by making a change of variables similar to the pure-gluon case, leading to

$$\text{sign}(\tau) \left(\det \Xi|_q \right)^4 \prod_{l=1}^k \int d\eta_{c_{\alpha_l}}^{A_l} \sum_{\substack{i=0 \\ i \notin \{\alpha_1, \dots, \alpha_k\}}}^{p+k} \left(\Xi|_q^{-1} \right)_{\bar{\beta}_l i} \sum_{j=1}^k \Xi_{i \alpha_j} \eta_{c_{\alpha_j}}^{B_l}. \quad (7.11)$$

Here $\Xi|_q$ refers to the elimination of all quark columns in the path-matrix. We can simplify the sum over i by making use of some basic facts of linear algebra. Namely, given a square matrix $M = (m_{ij})$ with minors M_{ij} , its determinant and inverse can be written as

$$\det M = \sum_i (-1)^{i+j} m_{ij} \det M_{ij} \quad \text{and} \quad (M^{-1})_{ij} = (-1)^{i+j} \frac{\det M_{ji}}{\det M}. \quad (7.12)$$

Hence, eq. (7.11) simplifies to

$$\text{sign}(\tau) \left(\det \Xi|_q \right)^{4-k} \prod_{l=1}^k \int d\eta_{c_{\alpha_l}}^{A_l} \sum_{j=1}^k \det \left(\Xi|_q (\bar{\beta}_l \rightarrow \alpha_j) \right) \eta_{c_{\alpha_j}}^{B_l}, \quad (7.13)$$

where $\Xi|_q (\bar{\beta}_l \rightarrow \alpha_j)$ denotes the replacement of an anti-quark column by a quark column. The remaining integrations are straightforward and give

$$\text{sign}(\tau) \left(\det \Xi|_q \right)^{4-k} \sum_{\sigma \in S_k} \text{sign}(\sigma) \prod_{i=1}^k \delta^{A_i B_{\sigma(i)}} \det \left(\Xi|_q (\bar{\beta}_{\sigma(i)} \rightarrow \alpha_i) \right). \quad (7.14)$$

The general $\mathcal{N} = 4$ super Yang-Mills $g^{n-2k} (q\bar{q})^k$ amplitude is therefore

$$A_{(q\bar{q})^k, n}^{\text{NPMHV}}(c_0, \dots, c_{\alpha_i}^{A_i}, \dots, c_{\bar{\beta}_j}^{B_j}, \dots, c_{p+k}, n) = \frac{\delta^{(4)}(p) \text{sign}(\tau)}{\langle 1 2 \rangle \langle 2 3 \rangle \dots \langle n 1 \rangle} \times \\ \sum_{\substack{\text{all paths} \\ \text{of length } p}} \left(\prod_{i=1}^p \tilde{R}_{n; \{I_i\}; a_i b_i}^{L_i; R_i} \right) \left(\det \Xi|_q \right)^{4-k} \sum_{\sigma \in S_k} \text{sign}(\sigma) \prod_{i=1}^k \delta^{A_i B_{\sigma(i)}} \det \left(\Xi|_q (\bar{\beta}_{\sigma(i)} \rightarrow \alpha_i) \right). \quad (7.15)$$

Note that during the derivation of this formula we assumed that there is at least one negative-helicity gluon. The only change in the case $k = p+2$ is that the η_n integration is no longer trivial and we put a gluino at position n . Hence, the path matrix has the size $(p+2) \times (2p+4)$ and eq. (7.15) still holds as its derivation did not depend on the matrix dimensions. Using (7.8) the

path matrix (4.12) then generalizes to the form

$$\Xi := \begin{pmatrix} 0 & \frac{\langle c_0 c_1 \rangle}{\langle c_0 n \rangle} & \frac{\langle c_0 c_2 \rangle}{\langle c_0 n \rangle} & \dots & \frac{\langle c_0 c_{p+k} \rangle}{\langle c_0 n \rangle} & 1 \\ \langle n c_0 \rangle & \langle n c_1 \rangle & \langle n c_2 \rangle & \dots & \langle n c_{p+k} \rangle & 0 \\ (\Xi_n)_{a_1 b_1}^{c_0} & (\Xi_n)_{a_1 b_1}^{c_1} & (\Xi_n)_{a_1 b_1}^{c_2} & \dots & (\Xi_n)_{a_1 b_1}^{c_{p+k}} & 0 \\ (\Xi_n)_{\{I_2\}; a_2 b_2}^{c_0} & (\Xi_n)_{\{I_2\}; a_2 b_2}^{c_1} & (\Xi_n)_{\{I_2\}; a_2 b_2}^{c_2} & \dots & (\Xi_n)_{\{I_2\}; a_2 b_2}^{c_{p+k}} & 0 \\ \vdots & \vdots & \vdots & \vdots & \vdots & \vdots \\ (\Xi_n)_{\{I_p\}; a_p b_p}^{c_0} & (\Xi_n)_{\{I_p\}; a_p b_p}^{c_1} & (\Xi_n)_{\{I_p\}; a_p b_p}^{c_2} & \dots & (\Xi_n)_{\{I_p\}; a_p b_p}^{c_{p+k}} & 0 \end{pmatrix}. \quad (7.16)$$

Generally the amplitudes take a more compact form if the gluino at position n is taken to be of helicity $-1/2$. Several explicit formulas for the MHV and NMHV cases can be found in Appendix B. In particular Appendix B.2.3 discusses a case without a negative helicity gluon at position n .

As we are interested in QCD tree amplitudes, we need to decouple possible intermediate scalar states arising from the Yukawa couplings $\tilde{g}_A \tilde{g}_B \phi^{AB}$ in the $\mathcal{N} = 4$ super Yang-Mills Lagrangian. As discussed in section 3, one case in which this can be achieved (although not the only one needed for QCD) is when the external fermion states all have the same flavor, due to the anti-symmetry of $\phi^{AB} = \epsilon^{ABCD} \phi_{CD}$. For this case, we specialize to $A_i = B_i = A$ for all external fermion legs i in our master formula (7.15), and perform the sum over permutations explicitly, yielding

$$A_{(q\bar{q})^k, n}^{\text{NPMHV}}(c_0, \dots, c_{\alpha_i}, \dots, c_{\beta_j}, \dots, c_{p+k}, n) = \frac{\delta^{(4)}(p) \text{sign}(\tau)}{\langle 1 2 \rangle \langle 2 3 \rangle \dots \langle n 1 \rangle} \sum_{\substack{\text{all paths} \\ \text{of length } p}} \left(\prod_{i=1}^p \tilde{R}_{n; \{I_i\}; a_i b_i}^{L_i; R_i} \right) \det \Xi(q \leftrightarrow \bar{q})|_{\bar{q}} \left(\det \Xi|_q \right)^3, \quad (7.17)$$

which reproduces eq. (5.2).

Acknowledgments

We thank Zvi Bern, Benedikt Biedermann, Jake Bourjaily, Harald Ita, Kemal Ozeren and Peter Uwer for helpful discussions. Several figures in this paper were made with JAXODRAW [40], based on AXODRAW [41]. This work was supported by the Volkswagen Foundation, and by the US Department of Energy under contract DE-AC02-76SF00515.

A Explicit formulae for gluon trees

Here we explicitly apply our formula (4.2) to the NMHV and NNMHV cases.

A.1 NMHV amplitudes

Without loss of generality, we take the negative-helicity gluons to be at positions c_0, c_1, n with $c_0 < c_1$. In the NMHV case only one path in figure 6 contributes and the path-matrix is a 2×2 matrix whose determinant we denote by $D_{n,a_1b_1}^{c_0c_1}$. Hence, the NMHV gluon amplitude is given by

$$A_n^{\text{NMHV}}(c_0^-, c_1^-, n^-) = \frac{\delta^{(4)}(p)}{\langle 1\ 2 \rangle \dots \langle n\ 1 \rangle} \sum_{2 \leq a_1 < b_1 \leq n-1} \tilde{R}_{n;a_1b_1} \cdot (D_{n,a_1b_1}^{c_0c_1})^4 \quad (\text{A.1})$$

where the determinant of the path-matrix is given explicitly by

$$D_{n,st}^{ab} := \begin{vmatrix} \langle n\ a \rangle & \langle n\ b \rangle \\ (\Xi_n)_{st}^a & (\Xi_n)_{st}^b \end{vmatrix} \stackrel{a \leq b}{=} \begin{cases} \langle n\ a \rangle \langle nts|b \rangle & a < s \leq b < t, \\ \langle n\ a \rangle \langle b\ n \rangle x_{st}^2 & a < s < t \leq b, \\ \langle b\ a \rangle \langle nts|n \rangle & s \leq a, b < t, \\ \langle n\ b \rangle \langle nst|a \rangle & s \leq a < t \leq b. \end{cases} \quad (\text{A.2})$$

For $a > b$ one can use the antisymmetry of the determinant, $D_{n,st}^{ab} = -D_{n,st}^{ba}$. Equation (A.2) is exactly the result we already stated in eq. (2.7). This formula is implemented in GGT by GGTnmhvgluon.

A.2 N²MHV amplitudes

The negative-helicity gluons are taken to be a^-, b^-, c^-, n^- with $a < b < c$, without loss of generality. According to figure 6 there are two contributing paths. Denoting the determinants of their corresponding path-matrices by D_1^{abc} and D_2^{abc} , the NNMHV gluon amplitude is given by

$$A_n^{\text{N}^2\text{MHV}}(a^-, b^-, c^-, n^-) = \frac{\delta^{(4)}(p)}{\langle 1\ 2 \rangle \dots \langle n\ 1 \rangle} \sum_{2 \leq a_1 < b_1 < n} \tilde{R}_{n;a_1b_1} \cdot \left[\sum_{a_1+1 \leq a_2 < b_2 \leq b_1} \tilde{R}_{n;b_1a_1;a_2b_2}^{0;a_1b_1} \cdot (D_1^{abc})^4 + \sum_{b_1 \leq a_2 < b_2 < n} \tilde{R}_{n;a_2b_2}^{a_1b_1;0} \cdot (D_2^{abc})^4 \right]. \quad (\text{A.3})$$

The explicit forms of the determinants of the path-matrices

$$D_1^{abc}(n, a_1, b_1, a_2, b_2) := \begin{vmatrix} \langle n\ a \rangle & \langle n\ b \rangle & \langle n\ c \rangle \\ (\Xi_n)_{a_1b_1}^a & (\Xi_n)_{a_1b_1}^b & (\Xi_n)_{a_1b_1}^c \\ (\Xi_n)_{b_1,a_1;a_2b_2}^a & (\Xi_n)_{b_1,a_1;a_2b_2}^b & (\Xi_n)_{b_1,a_1;a_2b_2}^c \end{vmatrix} \quad (\text{A.4})$$

and

$$D_2^{abc}(n, a_1, b_1, a_2, b_2) := \begin{vmatrix} \langle n\ a \rangle & \langle n\ b \rangle & \langle n\ c \rangle \\ (\Xi_n)_{a_1b_1}^a & (\Xi_n)_{a_1b_1}^b & (\Xi_n)_{a_1b_1}^c \\ (\Xi_n)_{a_2b_2}^a & (\Xi_n)_{a_2b_2}^b & (\Xi_n)_{a_2b_2}^c \end{vmatrix} \quad (\text{A.5})$$

are given by

$$D_1^{abc} = \left\{ \begin{array}{ll}
\langle a n \rangle \langle nb_1 a_1 | b \rangle \langle nb_1 a_1 b_2 a_2 | c \rangle & a < a_1 \leq b, c < b_1 \quad b < a_2 \leq c < b_2 \\
\langle n a \rangle \langle nb_1 a_1 | b \rangle \langle nb_1 a_1 | c \rangle x_{a_2 b_2}^2 & a < a_1 \leq b, c < b_1 \quad b < a_2, b_2 \leq c \\
\langle a n \rangle \langle b c \rangle \langle nb_1 a_1 a_2 b_2 | nb_1 a_1 \rangle & a < a_1 \leq b, c < b_1 \quad a_1 < a_2 \leq b, c < b_2 \\
\langle a n \rangle \langle nb_1 a_1 | c \rangle \langle nb_1 a_1 a_2 b_2 | b \rangle & a < a_1 \leq b, c < b_1 \quad a_1 < a_2 \leq b < b_2 \leq c \\
\langle n a \rangle \langle c n \rangle \langle nb_1 a_1 | b \rangle x_{a_1 b_1}^2 x_{a_2 b_2}^2 & a < a_1 \leq b < b_1 \leq c \quad b < a_2, b_2 \leq c \\
\langle n a \rangle \langle n c \rangle x_{a_1 b_1}^2 \langle nb_1 a_1 a_2 b_2 | b \rangle & a < a_1 \leq b < b_1 \leq c \quad a_2 \leq b < b_2 \\
\langle a b \rangle \langle nb_1 a_1 | n \rangle \langle nb_1 a_1 b_2 a_2 | c \rangle & a_1 \leq a, b, c < b_1 \quad b < a_2 \leq c < b_2 \\
\langle c b \rangle \langle nb_1 a_1 | n \rangle \langle nb_1 a_1 b_2 a_2 | a \rangle & a_1 \leq a, b, c < b_1 \quad a < a_2 \leq b, c < b_2 \\
\langle b a \rangle \langle nb_1 a_1 | n \rangle \langle nb_1 a_1 | c \rangle x_{a_2 b_2}^2 & a_1 \leq a, b, c < b_1 \quad b < a_2, b_2 \leq c \\
\langle nb_1 a_1 | n \rangle (x_{a_2 b_2}^2 \langle nb_1 a_1 | a \rangle \langle b c \rangle & a_1 \leq a, b, c < b_1 \quad a < a_2 \leq b < b_2 \leq c \\
\quad + \langle nb_1 a_1 a_2 b_2 | b \rangle \langle a c \rangle) & \\
\langle a b \rangle \langle nb_1 a_1 | n \rangle \langle nb_1 a_1 a_2 b_2 | c \rangle & a_1 \leq a, b, c < b_1 \quad a_2 \leq a, b < b_2 \leq c \\
\langle c b \rangle \langle nb_1 a_1 | n \rangle \langle nb_1 a_1 a_2 b_2 | a \rangle & a_1 \leq a, b, c < b_1 \quad a_1 < a_2 \leq a < b_2 \leq b \\
\langle b c \rangle \langle nb_1 a_1 | a \rangle \langle nb_1 a_1 | n \rangle x_{a_2 b_2} & a_1 \leq a, b, c < b_1 \quad a_1 < a_2 \leq a < b_2 \leq b \\
\langle c n \rangle \langle a b \rangle \langle na_1 | nb_1 \rangle x_{a_1 b_1}^2 x_{a_2 b_2}^2 & a_1 \leq a, b < b_1 \leq c \quad b < a_2, b_2 \leq b_1 \\
\langle c n \rangle (x_{a_2 b_2}^2 \langle nb_1 a_1 | a \rangle \langle na_1 b_1 | b \rangle & a_1 \leq a, b < b_1 \leq c \quad a < a_2 \leq b < b_2 \\
\quad + \langle na_1 b_1 | a \rangle \langle nb_1 a_1 a_2 b_2 | b \rangle) & \\
\langle n c \rangle \langle a b \rangle \langle nb_1 a_1 a_2 b_2 | na_1 b_1 \rangle & a_1 \leq a, b < b_1 \leq c \quad a_2 \leq a, b < b_2 \\
\langle c n \rangle \langle nb_1 a_1 | a \rangle \langle na_1 b_1 | b \rangle x_{a_2 b_2}^2 & a_1 \leq a, b < b_1 \leq c \quad a < a_2, b_2 \leq b \\
\langle n c \rangle \langle na_1 b_1 | b \rangle \langle nb_1 a_1 a_2 b_2 | a \rangle & a_1 \leq a, b < b_1 \leq c \quad a_2 \leq a < b_2 \leq b
\end{array} \right. \tag{A.6}$$

for $1 < a_1 < a_2 < b_2 \leq b_1 < n$ and

$$D_2^{abc} = \left\{ \begin{array}{ll}
\langle n a \rangle \langle nb_1 a_1 | b \rangle \langle nb_2 a_2 | c \rangle & a < a_1 \leq b < b_1 \leq c \quad a_2 \leq c < b_2 \\
\langle n a \rangle \langle c n \rangle \langle nb_1 a_1 | b \rangle x_{a_2 b_2}^2 & a < a_1 \leq b < b_1 \leq c \quad b_2 \leq c \\
\langle n a \rangle \langle b n \rangle \langle nb_2 a_2 | c \rangle x_{a_1 b_1}^2 & a < a_1, b_1 \leq b \quad b < a_2 \leq c < b_2 \\
\langle n a \rangle \langle b n \rangle \langle n c \rangle x_{a_1 b_1}^2 x_{a_2 b_2}^2 & a < a_1, b_1 \leq b \quad b < a_2, b_2 \leq c \\
\langle n a \rangle \langle b c \rangle \langle nb_2 a_2 | n \rangle x_{a_1 b_1}^2 & a < a_1, b_1 \leq b \quad a_2 \leq b, c < b_2 \\
\langle n a \rangle \langle c n \rangle \langle nb_2 a_2 | b \rangle x_{a_1 b_1}^2 & a < a_1, b_1 \leq b \quad a_2 \leq b < b_2 \leq c \\
\langle a b \rangle \langle na_1 b_1 | n \rangle \langle nb_2 a_2 | c \rangle & a_1 \leq a, b < b_1 \leq c \quad a_2 \leq c < b_2 \\
\langle c n \rangle \langle a b \rangle \langle na_1 b_1 | n \rangle x_{a_2 b_2}^2 & a_1 \leq a, b < b_1 \leq c \quad b_2 \leq c \\
\langle n b \rangle \langle na_1 b_1 | a \rangle \langle nb_2 a_2 | c \rangle & a_1 \leq a < b_1 \leq b \quad b < a_2 \leq c < b_2 \\
\langle n b \rangle \langle c n \rangle \langle na_1 b_1 | a \rangle x_{a_2 b_2}^2 & a_1 \leq a < b_1 \leq b \quad b < a_2, b_2 \leq c \\
\langle c b \rangle \langle na_1 b_1 | a \rangle \langle nb_2 a_2 | n \rangle & a_1 \leq a < b_1 \leq b \quad a_2 \leq b, c < b_2 \\
\langle n c \rangle \langle na_1 b_1 | a \rangle \langle na_2 b_2 | b \rangle & a_1 \leq a < b_1 \leq b \quad a_2 \leq b < b_2 \leq c
\end{array} \right. \tag{A.7}$$

for $1 < a_1 < b_1 \leq a_2 < b_2 < n$. For other orderings of a, b, c one can use the total antisymmetry of D_1^{abc} and D_2^{abc} under permutations of a, b, c . It is quite astonishing that in 28 out of 30 cases these determinants are given by a single term. This formula is implemented in GGT by GGTnnmhvg1uon.

B Explicit formulae for trees with fermions

Here we explicitly write out our formulas (5.2) and (6.2) for the MHV, NMHV and NNMHV cases with up to six fermions.

B.1 MHV amplitudes

The simplest amplitudes involving fermions are the MHV amplitudes. The amplitudes with one negative-helicity gluon a and two fermions of opposite helicity and the same flavor, $b (+\frac{1}{2})$ and $\bar{c} (-\frac{1}{2})$ (or vice-versa), are given by

$$A_n(a^-, b, \bar{c}) = \delta^{(4)}(p) \frac{\langle a c \rangle^3 \langle a b \rangle}{\langle 1 2 \rangle \dots \langle n 1 \rangle}, \quad (\text{B.1})$$

$$A_n(a^-, \bar{b}, c) = -\delta^{(4)}(p) \frac{\langle a b \rangle^3 \langle a c \rangle}{\langle 1 2 \rangle \dots \langle n 1 \rangle}. \quad (\text{B.2})$$

These formulae correspond to case (1) in figure 3. We note that the latter formula is related to the former one by a reflection symmetry, under which the cyclic ordering is reversed and there is a relabeling $b \leftrightarrow c$. In the NMHV case we will omit formulae that can be obtained from the presented formulae by a reflection symmetry.

An equally compact formula can be obtained for the MHV amplitudes with four fermions and only positive-helicity gluons:

$$A_n(a^A, \bar{b}^B, c^C, \bar{d}^D) = \frac{\delta^{(4)}(p) \langle b d \rangle^2}{\langle 1 2 \rangle \dots \langle n 1 \rangle} (\delta^{AB} \delta^{CD} \langle d a \rangle \langle c b \rangle - \delta^{AD} \delta^{BC} \langle d c \rangle \langle a b \rangle), \quad (\text{B.3})$$

$$A_n(a^A, b^B, \bar{c}^C, \bar{d}^D) = \frac{\delta^{(4)}(p) \langle c d \rangle^2}{\langle 1 2 \rangle \dots \langle n 1 \rangle} (\delta^{AD} \delta^{BC} \langle d b \rangle \langle a c \rangle - \delta^{AC} \delta^{BD} \langle d a \rangle \langle b c \rangle), \quad (\text{B.4})$$

which in the single-flavor case simplifies to

$$A_n(a, \bar{b}, c, \bar{d}) = \frac{\delta^{(4)}(p) \langle b d \rangle^3 \langle a c \rangle}{\langle 1 2 \rangle \dots \langle n 1 \rangle}, \quad (\text{B.5})$$

$$A_n(a, b, \bar{c}, \bar{d}) = -\frac{\delta^{(4)}(p) \langle c d \rangle^3 \langle a b \rangle}{\langle 1 2 \rangle \dots \langle n 1 \rangle}. \quad (\text{B.6})$$

Equation (B.6) corresponds to case (2a) in figure 3, whereas eq. (B.3) for $A = B \neq C = D$ corresponds to case (2b).

To complete the list of MHV amplitudes with up to four fermions we also give the MHV amplitude with four positive-helicity fermions and one negative-helicity gluon:

$$\begin{aligned}
A_n(a^A, b^B, c^C, d^D, n^-) &= \int d\eta_a^A \int d\eta_b^B \int d\eta_c^C \int d\eta_d^D \int d^4\eta_n \mathcal{A}_n^{\text{MHV}} \\
&= \frac{\delta^{(4)}(p)\epsilon^{ABCD}}{\langle 1 2 \rangle \dots \langle n 1 \rangle} \langle n a \rangle \langle n b \rangle \langle n c \rangle \langle n d \rangle.
\end{aligned} \tag{B.7}$$

This amplitude is not needed for QCD.

B.2 NMHV amplitudes

B.2.1 Two fermions

To illustrate the use of our master formula (5.2) we compute the NMHV amplitude with two opposite-helicity fermions at positions a, \bar{b} and two negative-helicity gluons at positions c and n . At this stage we leave the color order arbitrary. Starting with the path-matrix

$$\Xi^{\text{path}} = \begin{pmatrix} \langle n c \rangle & \langle n a \rangle & \langle n \bar{b} \rangle \\ (\Xi_n)_c^{st} & (\Xi_n)_a^{st} & (\Xi_n)_{\bar{b}}^{st} \end{pmatrix} \tag{B.8}$$

we can immediately write down the amplitude

$$(A_n)_{q\bar{q}}^{\text{NMHV}} = \frac{\delta^{(4)}(p) \text{sign}(\tau)}{\langle 1 2 \rangle \dots \langle n 1 \rangle} \sum_{1 < s < t < n} \tilde{R}_{n;st} D_{n;st}^{ca} \left(D_{n;st}^{c\bar{b}} \right)^3, \tag{B.9}$$

where the 2×2 determinant $D_{n;st}^{ab}$ has been defined in eq. (A.2). As already stated, the last equation holds for an arbitrary color ordering. In the following we take $a < b < c$ and specify the color ordering:

$$\begin{aligned}
A_n(a, b^-, \bar{c}, n^-) &= \frac{\delta^{(4)}(p)}{\langle 1 2 \rangle \dots \langle n 1 \rangle} \left[- \langle a b \rangle \langle b c \rangle^3 \sum_{1 < s \leq a, b, c < t < n} \langle nts|n \rangle^4 \tilde{R}_{n,st} \right. \\
&\quad - \langle b c \rangle^3 \langle a n \rangle \sum_{a < s \leq b, c < t < n} \langle nts|b \rangle \langle nts|n \rangle^3 \tilde{R}_{n,st} \\
&\quad - \langle c n \rangle^3 \langle a n \rangle \sum_{a < s \leq b < t \leq c} \langle nst|b \rangle^3 \langle nts|b \rangle \tilde{R}_{n,st} \\
&\quad \left. - \langle c n \rangle^3 \langle a b \rangle \sum_{1 < s \leq a, b < t \leq c} \langle nst|b \rangle^3 \langle nts|n \rangle \tilde{R}_{n,st} \right], \tag{B.10}
\end{aligned}$$

$$A_n(a, \bar{b}, c^-, n^-) = \frac{\delta^{(4)}(p)}{\langle 1 2 \rangle \dots \langle n 1 \rangle} \left[+ \langle a c \rangle \langle b c \rangle^3 \sum_{1 < s \leq a, b, c < t < n} \langle nts|n \rangle^4 \tilde{R}_{n,st} \right.$$

$$\begin{aligned}
& + \langle a n \rangle \langle b n \rangle^3 \sum_{b < s \leq c < t < n} \langle nts|c \rangle^4 \tilde{R}_{n,st} \\
& + \langle n c \rangle^4 \langle a n \rangle \langle b n \rangle^3 \sum_{b < s < t \leq c} (x_{st}^2)^4 \tilde{R}_{n,st} \\
& + \langle c n \rangle^4 \sum_{1 < s \leq a, b < t \leq c} \langle nst|b \rangle^3 \langle nst|a \rangle \tilde{R}_{n,st} \\
& + \langle b c \rangle^3 \langle a n \rangle \sum_{a < s \leq b, c < t < n} \langle nts|c \rangle \langle nts|n \rangle^3 \tilde{R}_{n,st} \\
& + \langle c n \rangle^4 \langle a n \rangle \sum_{a < s \leq b < t \leq c} x_{st}^2 \langle nst|b \rangle^3 \tilde{R}_{n,st} \Big]. \quad (\text{B.11})
\end{aligned}$$

These simplified expressions are implemented in GGT by GGTnmhv2ferm (see appendix C).

B.2.2 Four Fermions

We proceed with the NMHV amplitude with four fermions at positions $a_1^{A_1}, a_2^{A_2}, \bar{b}_1^{B_1}, \bar{b}_2^{B_2}$ and one negative-helicity gluon. Without loss of generality we put the negative-helicity gluon at position n . Again we leave the color ordering arbitrary. A straightforward application of our formulas (6.2) and (5.2) yields

$$(A_n)_{(q\bar{q})^2}^{\text{NMHV}} = \frac{\delta^{(4)}(p) \text{sign}(\tau)}{\langle 1 2 \rangle \dots \langle n 1 \rangle} \sum_{1 < s < t < n} \tilde{R}_{n,st} \left(D_{n,st}^{\bar{b}_1 \bar{b}_2} \right)^2 \left(\delta^{A_1 B_1} \delta^{A_2 B_2} D_{n,st}^{a_1 \bar{b}_2} D_{n,st}^{\bar{b}_1 a_2} - \delta^{A_1 B_2} \delta^{A_2 B_1} D_{n,st}^{a_2 \bar{b}_2} D_{n,st}^{\bar{b}_1 a_1} \right) \quad (\text{B.12})$$

in the $\mathcal{N} = 4$ super Yang-Mills case, and

$$(A_n)_{(q\bar{q})^2}^{\text{NMHV}} = \frac{\delta^{(4)}(p) \text{sign}(\tau)}{\langle 1 2 \rangle \dots \langle n 1 \rangle} \sum_{1 < s < t < n} \tilde{R}_{n,st} \left(D_{n,st}^{\bar{b}_1 \bar{b}_2} \right)^3 D_{n,st}^{a_1 a_2} \quad (\text{B.13})$$

for single-flavor QCD, with $D_{n,st}^{ab}$ defined in equation (A.2). Taking $a < b < c < d$ we now specify the color ordering,

$$\begin{aligned}
A_n(a^A, b^B, \bar{c}^C, \bar{d}^D, n^-) &= \frac{\delta^{(4)}(p)}{\langle 1 2 \rangle \dots \langle n 1 \rangle} \times \\
& \times \left[+ \delta^{AC} \delta^{BD} \langle a n \rangle \langle b c \rangle \langle c d \rangle^2 \sum_{a < s \leq b, d < t < n} \langle nts|d \rangle \langle nts|n \rangle^3 \tilde{R}_{n,st} - (c \leftrightarrow d) \right. \\
& + \delta^{AC} \delta^{BD} \langle a d \rangle \langle b c \rangle \langle d c \rangle^2 \sum_{1 < s \leq a, d < t < n} \langle nts|n \rangle^4 \tilde{R}_{n,st} - (a \leftrightarrow b) \\
& \left. + \delta^{AC} \delta^{BD} \langle n a \rangle \langle b c \rangle \langle d n \rangle^3 \sum_{a < s \leq b, c < t \leq d} x_{st}^2 \langle nst|n \rangle \langle nst|c \rangle^2 \tilde{R}_{n,st} \right]
\end{aligned}$$

$$\begin{aligned}
& - \delta^{AD} \delta^{BC} \langle a n \rangle \langle d n \rangle^3 \sum_{a < s \leq b, c < t \leq d} \langle nts|c \rangle \langle nst|b \rangle \langle nst|c \rangle^2 \tilde{R}_{n,st} \\
& + \delta^{AC} \delta^{BD} \langle b c \rangle \langle d n \rangle^3 \sum_{1 < s \leq a, c < t \leq d} \langle nst|a \rangle \langle nts|n \rangle \langle nst|c \rangle^2 \tilde{R}_{n,st} - (a \leftrightarrow b) \Big], \tag{B.14}
\end{aligned}$$

where “ $(c \leftrightarrow d)$ ” implies the substitution $c \leftrightarrow d$ in the arguments of the spinor strings, as well as the corresponding substitution $C \leftrightarrow D$ in the arguments of the δ functions, but *no* change in the summation range. The other inequivalent orderings of quarks and anti-quarks are,

$$\begin{aligned}
A_n(a^A, \bar{b}^B, c^C, \bar{d}^D, n^-) &= \frac{\delta^{(4)}(p)}{\langle 1 2 \rangle \dots \langle n 1 \rangle} \times \\
& \times \Big[+ \delta^{AB} \delta^{CD} \langle a n \rangle \langle b n \rangle^3 \sum_{b < s \leq c, d < t < n} \langle nts|c \rangle \langle nts|d \rangle^3 \tilde{R}_{n,st} \\
& + \delta^{AB} \delta^{CD} \langle n a \rangle \langle c b \rangle \langle b d \rangle^2 \sum_{a < s \leq b, d < t < n} \langle nts|d \rangle \langle nts|n \rangle^3 \tilde{R}_{n,st} - (b \leftrightarrow d) \\
& + \delta^{AB} \delta^{CD} \langle a d \rangle \langle b c \rangle \langle d b \rangle^2 \sum_{1 < s \leq a, d < t < n} \langle nts|n \rangle^4 \tilde{R}_{n,st} - (a \leftrightarrow c) \\
& + \delta^{AB} \delta^{CD} \langle n a \rangle \langle d n \rangle^3 \langle n b \rangle^3 \sum_{b < s \leq c < t \leq d} \langle nts|c \rangle (x_{st}^2)^3 \tilde{R}_{n,st} \\
& + \delta^{AB} \delta^{CD} \langle n a \rangle \langle n c \rangle \langle n b \rangle^3 \langle n d \rangle^3 \sum_{b < s < t \leq c} (x_{st}^2)^4 \tilde{R}_{n,st} \\
& + \delta^{AB} \delta^{CD} \langle n a \rangle \langle b c \rangle \langle d n \rangle^3 \sum_{a < s \leq b, c < t \leq d} x_{st}^2 \langle nst|n \rangle \langle nst|b \rangle^2 \tilde{R}_{n,st} \\
& - \delta^{AD} \delta^{CB} \langle n a \rangle \langle d n \rangle^3 \sum_{a < s \leq b, c < t \leq d} \langle nts|b \rangle \langle nst|c \rangle \langle nst|b \rangle^2 \tilde{R}_{n,st} \\
& + \delta^{AB} \delta^{CD} \langle n a \rangle \langle n c \rangle \langle d n \rangle^3 \sum_{a < s \leq b < t \leq c} x_{st}^2 \langle nst|b \rangle^3 \tilde{R}_{n,st} \\
& + \delta^{AB} \delta^{CD} \langle b c \rangle \langle d n \rangle^3 \sum_{1 < s \leq a, c < t \leq d} \langle nst|a \rangle \langle nts|n \rangle \langle nst|b \rangle^2 \tilde{R}_{n,st} - (a \leftrightarrow c) \\
& + \delta^{AB} \delta^{CD} \langle n c \rangle \langle n d \rangle^3 \sum_{1 < s \leq a, b < t \leq c} \langle nst|a \rangle \langle nst|b \rangle^3 \tilde{R}_{n,st} \Big], \tag{B.15}
\end{aligned}$$

$$A_n(a^A, \bar{b}^B, \bar{c}^C, d^D, n^-) = - \frac{\delta^{(4)}(p)}{\langle 1 2 \rangle \dots \langle n 1 \rangle} \times$$

$$\begin{aligned}
& \times \left[+ \delta^{AB} \delta^{CD} \langle a n \rangle \langle b n \rangle^3 \sum_{b < s \leq c, d < t < n} \langle nts|d \rangle \langle nts|c \rangle^3 \tilde{R}_{n,st} \right. \\
& + \delta^{AB} \delta^{CD} \langle n a \rangle \langle n d \rangle \langle b n \rangle^3 \sum_{b < s \leq c < t \leq d} x_{st}^2 \langle nts|c \rangle^3 \tilde{R}_{n,st} \\
& + \delta^{AB} \delta^{CD} \langle n a \rangle \langle d b \rangle \langle b c \rangle^2 \sum_{a < s \leq b, d < t < n} \langle nts|c \rangle \langle nts|n \rangle^3 \tilde{R}_{n,st} - (b \leftrightarrow c) \\
& + \delta^{AB} \delta^{CD} \langle n a \rangle \langle n d \rangle \langle b c \rangle^2 \sum_{a < s \leq b, c < t \leq d} \langle nts|c \rangle \langle nst|b \rangle \langle nts|n \rangle^2 \tilde{R}_{n,st} - (b \leftrightarrow c) \\
& + \delta^{AB} \delta^{CD} \langle a c \rangle \langle b d \rangle \langle c b \rangle^2 \sum_{1 < s \leq a, d < t < n} \langle nts|n \rangle^4 \tilde{R}_{n,st} - (a \leftrightarrow d) \\
& + \delta^{AB} \delta^{CD} \langle a c \rangle \langle n d \rangle \langle c b \rangle^2 \sum_{1 < s \leq a, c < t \leq d} \langle nst|b \rangle \langle nst|n \rangle^3 \tilde{R}_{n,st} - (b \leftrightarrow c) \\
& + \delta^{AB} \delta^{CD} \langle n a \rangle \langle n d \rangle \langle n b \rangle^3 \langle n c \rangle^3 \sum_{b < s < t \leq c} (x_{st}^2)^4 \tilde{R}_{n,st} \\
& + \delta^{AB} \delta^{CD} \langle n a \rangle \langle n d \rangle \langle c n \rangle^3 \sum_{a < s \leq b < t \leq c} x_{st}^2 \langle nst|b \rangle^3 \tilde{R}_{n,st} \\
& \left. + \delta^{AB} \delta^{CD} \langle n d \rangle \langle n c \rangle^3 \sum_{1 < s \leq a, b < t \leq c} \langle nst|a \rangle \langle nst|b \rangle^3 \tilde{R}_{n,st} \right], \tag{B.16}
\end{aligned}$$

$$\begin{aligned}
A_n(\bar{a}^A, b^B, c^C, \bar{d}^D, n^-) &= -\frac{\delta^{(4)}(p)}{\langle 1 2 \rangle \dots \langle n 1 \rangle} \times \\
& \times \left[+ \delta^{AB} \delta^{CD} \langle b n \rangle \langle a n \rangle^3 \sum_{b < s \leq c, d < t < n} \langle nts|c \rangle \langle nts|d \rangle^3 \tilde{R}_{n,st} \right. \\
& + \delta^{AB} \delta^{CD} \langle b d \rangle \langle a n \rangle^3 \sum_{a < s \leq b, d < t < n} \langle nts|n \rangle \langle nts|c \rangle \langle nts|d \rangle^2 \tilde{R}_{n,st} - (b \leftrightarrow c) \\
& + \delta^{AB} \delta^{CD} \langle b d \rangle \langle a c \rangle \langle d a \rangle^2 \sum_{1 < s \leq a, d < t < n} \langle nts|n \rangle^4 \tilde{R}_{n,st} - (b \leftrightarrow c) \\
& + \delta^{AB} \delta^{CD} \langle n b \rangle \langle d n \rangle^3 \langle n a \rangle^3 \sum_{b < s \leq c < t \leq d} \langle nts|c \rangle (x_{st}^2)^3 \tilde{R}_{n,st} \\
& + \delta^{AB} \delta^{CD} \langle n b \rangle \langle n c \rangle \langle n a \rangle^3 \langle n d \rangle^3 \sum_{b < s < t \leq c} (x_{st}^2)^4 \tilde{R}_{n,st} \\
& \left. + \delta^{AB} \delta^{CD} \langle n a \rangle^3 \langle n d \rangle^3 \sum_{a < s \leq b, c < t \leq d} \langle nst|b \rangle \langle nts|c \rangle (x_{st}^2)^2 \tilde{R}_{n,st} - (b \leftrightarrow c) \right]
\end{aligned}$$

$$\begin{aligned}
& + \delta^{AB} \delta^{CD} \langle n c \rangle \langle d n \rangle^3 \langle n a \rangle^3 \sum_{a < s \leq b < t \leq c} \langle nst|b \rangle (x_{st}^2)^3 \tilde{R}_{n,st} \\
& + \delta^{AB} \delta^{CD} \langle a c \rangle \langle d n \rangle^3 \sum_{1 < s \leq a, c < t \leq d} \langle nst|b \rangle \langle nts|n \rangle \langle nst|a \rangle^2 \tilde{R}_{n,st} - (b \leftrightarrow c) \\
& + \delta^{AB} \delta^{CD} \langle n c \rangle \langle n d \rangle^3 \sum_{1 < s \leq a, b < t \leq c} \langle nst|b \rangle \langle nst|a \rangle^3 \tilde{R}_{n,st} \Big]. \tag{B.17}
\end{aligned}$$

For $A \neq B$, and all fermions cyclically adjacent we have

$$\begin{aligned}
A_n(a^A, \overline{(a+1)^B}, (a+2)^B, \overline{(a+3)^A}, n^-) &= \frac{\delta^{(4)}(p)}{\langle 1 2 \rangle \dots \langle n 1 \rangle} \times \\
& \left[\langle a n \rangle \langle a+2 a+3 \rangle \langle a+1 a+3 \rangle^2 \sum_{a+3 < t < n} \langle nta+2|a+1 \rangle \langle nta+1|n \rangle^3 \tilde{R}_{n,a+1t} \right. \\
& + \langle a+2 a+3 \rangle \langle a a+1 \rangle \langle a+1 a+3 \rangle^2 \sum_{1 < s \leq a, a+3 < t < n} \langle nts|n \rangle^4 \tilde{R}_{n,st} \\
& + \langle a n \rangle \langle a+3 n \rangle^3 \langle a+1 a+2 \rangle^4 \langle n|x_{n,a+3}|a+2 \rangle \langle n|x_{n,a+1}|a+1 \rangle \langle n|x_{n,a+1}|a+2 \rangle^2 \tilde{R}_{n,a+1a+3} \\
& \left. - \langle a a+1 \rangle \langle a+3 n \rangle^3 \sum_{1 < s \leq a} \langle nsa+3|a+2 \rangle \langle nsa+3|n \rangle \langle nsa+3|a+1 \rangle^2 \tilde{R}_{n,sa+3} \right]. \tag{B.18}
\end{aligned}$$

This amplitude may be used to generate the NMHV amplitudes for $Vq\bar{q}g \dots g$, as discussed in section 3.

In the single-flavor case we obtain

$$\begin{aligned}
A_n(a, b, \bar{c}, \bar{d}, n^-) &= \frac{\delta^{(4)}(p)}{\langle 1 2 \rangle \dots \langle n 1 \rangle} \left[+ \langle n a \rangle \langle c d \rangle^3 \sum_{a < s \leq b, d < t < n} \langle nts|b \rangle \langle nts|n \rangle^3 \tilde{R}_{n,st} \right. \\
& + \langle a b \rangle \langle d c \rangle^3 \sum_{1 < s \leq a, d < t < n} \langle nts|n \rangle^4 \tilde{R}_{n,st} \\
& + \langle n a \rangle \langle d n \rangle^3 \sum_{a < s \leq b, c < t \leq d} \langle nts|b \rangle \langle nst|c \rangle^3 \tilde{R}_{n,st} \\
& \left. + \langle b a \rangle \langle d n \rangle^3 \sum_{1 < s \leq a, c < t \leq d} \langle nts|n \rangle \langle nst|c \rangle^3 \tilde{R}_{n,st} \right], \tag{B.19}
\end{aligned}$$

$$\begin{aligned}
A_n(a, \bar{b}, c, \bar{d}, n^-) &= \frac{\delta^{(4)}(p)}{\langle 1 2 \rangle \dots \langle n 1 \rangle} \left[+ \langle a n \rangle \langle b n \rangle^3 \sum_{b < s \leq c, d < t < n} \langle nts|c \rangle \langle nts|d \rangle^3 \tilde{R}_{n,st} \right. \\
& + \langle n a \rangle \langle d b \rangle^3 \sum_{a < s \leq b, d < t < n} \langle nts|c \rangle \langle nts|n \rangle^3 \tilde{R}_{n,st} \\
& \left. \right]
\end{aligned}$$

$$\begin{aligned}
& + \langle a c \rangle \langle b d \rangle^3 \sum_{1 < s \leq a, d < t < n} \langle nts|n \rangle^4 \tilde{R}_{n,st} \\
& + \langle n a \rangle \langle d n \rangle^3 \langle n b \rangle^3 \sum_{b < s \leq c < t \leq d} \langle nts|c \rangle (x_{st}^2)^3 \tilde{R}_{n,st} \\
& + \langle n a \rangle \langle n c \rangle \langle n b \rangle^3 \langle n d \rangle^3 \sum_{b < s < t \leq c} (x_{st}^2)^4 \tilde{R}_{n,st} \\
& + \langle n a \rangle \langle n d \rangle^3 \sum_{a < s \leq b, c < t \leq d} \langle nts|c \rangle \langle nst|b \rangle^3 \tilde{R}_{n,st} \\
& + \langle n a \rangle \langle n c \rangle \langle d n \rangle^3 \sum_{a < s \leq b < t \leq c} x_{st}^2 \langle nst|b \rangle^3 \tilde{R}_{n,st} \\
& + \langle a c \rangle \langle d n \rangle^3 \sum_{1 < s \leq a, c < t \leq d} \langle nts|n \rangle \langle nst|b \rangle^3 \tilde{R}_{n,st} \\
& + \langle n c \rangle \langle n d \rangle^3 \sum_{1 < s \leq a, b < t \leq c} \langle nst|a \rangle \langle nst|b \rangle^3 \tilde{R}_{n,st} \Big], \quad (\text{B.20})
\end{aligned}$$

$$\begin{aligned}
A_n(a, \bar{b}, \bar{c}, d, n^-) = & -\frac{\delta^{(4)}(p)}{\langle 1 2 \rangle \dots \langle n 1 \rangle} \Big[+ \langle a n \rangle \langle b n \rangle^3 \sum_{b < s \leq c, d < t < n} \langle nts|d \rangle \langle nts|c \rangle^3 \tilde{R}_{n,st} \\
& + \langle n a \rangle \langle n d \rangle \langle b n \rangle^3 \sum_{b < s \leq c < t \leq d} x_{st}^2 \langle nts|c \rangle^3 \tilde{R}_{n,st} \\
& + \langle n a \rangle \langle c b \rangle^3 \sum_{a < s \leq b, d < t < n} \langle nts|d \rangle \langle nts|n \rangle^3 \tilde{R}_{n,st} \\
& + \langle n a \rangle \langle n d \rangle \langle b c \rangle^3 \sum_{a < s \leq b, c < t \leq d} x_{st}^2 \langle nts|n \rangle^3 \tilde{R}_{n,st} \\
& + \langle a d \rangle \langle b c \rangle^3 \sum_{1 < s \leq a, d < t < n} \langle nts|n \rangle^4 \tilde{R}_{n,st} \\
& + \langle b c \rangle^3 \langle n d \rangle \sum_{1 < s \leq a, c < t \leq d} \langle nst|a \rangle \langle nst|n \rangle^3 \tilde{R}_{n,st} \\
& + \langle n a \rangle \langle n d \rangle \langle n b \rangle^3 \langle n c \rangle^3 \sum_{b < s < t \leq c} (x_{st}^2)^4 \tilde{R}_{n,st} \\
& + \langle n a \rangle \langle n d \rangle \langle c n \rangle^3 \sum_{a < s \leq b < t \leq c} x_{st}^2 \langle nst|b \rangle^3 \tilde{R}_{n,st}
\end{aligned}$$

$$+ \langle n d \rangle \langle n c \rangle^3 \sum_{1 < s \leq a, b < t \leq c} \langle nst|a \rangle \langle nst|b \rangle^3 \tilde{R}_{n,st} \Big], \quad (\text{B.21})$$

$$\begin{aligned} A_n(\bar{a}, b, c, \bar{d}, n^-) = & -\frac{\delta^{(4)}(p)}{\langle 1 2 \rangle \dots \langle n 1 \rangle} \Bigg[+ \langle b n \rangle \langle a n \rangle^3 \sum_{b < s \leq c, d < t < n} \langle nts|c \rangle \langle nts|d \rangle^3 \tilde{R}_{n,st} \\ & + \langle b c \rangle \langle a n \rangle^3 \sum_{a < s \leq b, d < t < n} \langle nts|n \rangle \langle nts|d \rangle^3 \tilde{R}_{n,st} \\ & + \langle b c \rangle \langle a d \rangle^3 \sum_{1 < s \leq a, d < t < n} \langle nts|n \rangle^4 \tilde{R}_{n,st} \\ & + \langle n b \rangle \langle d n \rangle^3 \langle n a \rangle^3 \sum_{b < s \leq c < t \leq d} \langle nts|c \rangle (x_{st}^2)^3 \tilde{R}_{n,st} \\ & + \langle n b \rangle \langle n c \rangle \langle n a \rangle^3 \langle n d \rangle^3 \sum_{b < s < t \leq c} (x_{st}^2)^4 \tilde{R}_{n,st} \\ & + \langle n a \rangle^3 \langle n d \rangle^3 \langle b c \rangle \sum_{a < s \leq b, c < t \leq d} \langle nts|n \rangle (x_{st}^2)^3 \tilde{R}_{n,st} \\ & + \langle n c \rangle \langle d n \rangle^3 \langle n a \rangle^3 \sum_{a < s \leq b < t \leq c} \langle nst|b \rangle (x_{st}^2)^3 \tilde{R}_{n,st} \\ & + \langle b c \rangle \langle d n \rangle^3 \sum_{1 < s \leq a, c < t \leq d} \langle nts|n \rangle \langle nst|a \rangle^3 \tilde{R}_{n,st} \\ & + \langle n c \rangle \langle n d \rangle^3 \sum_{1 < s \leq a, b < t \leq c} \langle nst|b \rangle \langle nst|a \rangle^3 \tilde{R}_{n,st} \Big]. \quad (\text{B.22}) \end{aligned}$$

These simplified expressions are implemented in GGT by `GGTnmhv4fermS` for the single-flavor case, and by `GGTnmhv4ferm` for the general-flavor case. See appendix C for the documentation.

B.2.3 Six fermions

In the case of the six-fermion NMHV amplitude there is no negative-helicity gluon for us to put at position n as we did in the previous examples. The fermions are at positions $a_1^{A_1}, a_2^{A_2}, a_3^{A_3}, \bar{b}_1^{B_1}, \bar{b}_2^{B_2}$ and \bar{n}^{B_3} . This time the path-matrix (7.16) is given by

$$\Xi^{\text{path}} = \begin{pmatrix} \frac{\langle \bar{b}_2 \bar{b}_1 \rangle}{\langle \bar{b}_2 n \rangle} & 0 & 1 & \frac{\langle \bar{b}_2 a_1 \rangle}{\langle \bar{b}_2 n \rangle} & \frac{\langle \bar{b}_2 a_2 \rangle}{\langle \bar{b}_2 n \rangle} & \frac{\langle \bar{b}_2 a_3 \rangle}{\langle \bar{b}_2 n \rangle} \\ \langle n \bar{b}_1 \rangle & \langle n \bar{b}_2 \rangle & 0 & \langle n a_1 \rangle & \langle n a_2 \rangle & \langle n a_3 \rangle \\ (\Xi_n)_{st}^{\bar{b}_1} & (\Xi_n)_{st}^{\bar{b}_2} & 0 & (\Xi_n)_{st}^{a_1} & (\Xi_n)_{st}^{a_2} & (\Xi_n)_{st}^{a_3} \end{pmatrix}. \quad (\text{B.23})$$

As ingredients of formula (6.2) we need the determinants

$$\det(\Xi^{\text{path}}|_q) = D_{n;st}^{\bar{b}_1 \bar{b}_2}, \quad \det(\Xi^{\text{path}}|_q(\bar{b}_1 \rightarrow a_i)) = D_{n;st}^{a_i \bar{b}_2}, \quad (\text{B.24})$$

$$\det(\Xi^{\text{path}}|_q(\bar{b}_2 \rightarrow a_i)) = D_{n;st}^{\bar{b}_1 a_i}, \quad \det(\Xi^{\text{path}}|_q(\bar{n} \rightarrow a_i)) = D_{n;st}^{\bar{b}_1 \bar{b}_2 a_i}. \quad (\text{B.25})$$

We recall that $D_{n;st}^{ab}$ has been defined in eq. (A.2) and the 3×3 determinant $D_{n;st}^{abc}$ reads

$$D_{n;st}^{abc} := \begin{vmatrix} \frac{\langle b a \rangle}{\langle b n \rangle} & 0 & \frac{\langle b c \rangle}{\langle b n \rangle} \\ \langle n a \rangle & \langle n b \rangle & \langle n c \rangle \\ (\Xi_n)_{st}^a & (\Xi_n)_{st}^b & (\Xi_n)_{st}^c \end{vmatrix} = \langle a b \rangle (\Xi_n)_{st}^c + \langle b c \rangle (\Xi_n)_{st}^a + \langle c a \rangle (\Xi_n)_{st}^b. \quad (\text{B.26})$$

For $a < b < c$ we have

$$D_{n;st}^{abc} = \begin{cases} \langle a b \rangle \langle nts|c \rangle & b < s \leq c < t \\ \langle a b \rangle \langle c n \rangle x_{st}^2 & b < s < t \leq c \\ \langle nts|a \rangle \langle c b \rangle & a < s \leq b, c < t \\ \langle n a \rangle \langle b c \rangle x_{st}^2 & a < s < t \leq b \\ \langle a b \rangle \langle c n \rangle x_{st}^2 - \langle a c \rangle \langle nts|b \rangle & a < s \leq b < t \leq c \\ \langle a b \rangle \langle nst|c \rangle & s \leq a, b < t \leq c \\ \langle c b \rangle \langle nst|a \rangle & s \leq a < t \leq b, \end{cases} \quad (\text{B.27})$$

and $D_{n;st}^{abc}$ is totally antisymmetric in a, b, c . Thus, the $\mathcal{N} = 4$ super Yang-Mills NMHV six-fermion amplitude is

$$(A_n)_{(q\bar{q})^3}^{\text{NMHV}} = \frac{\delta^{(4)}(p) \text{sign}(\tau)}{\langle 1 2 \rangle \dots \langle n 1 \rangle} \sum_{1 < s < t < n} \tilde{R}_{n;st} D_{n;st}^{\bar{b}_1 \bar{b}_2} \left(\begin{aligned} & + \delta^{A_1 B_1} \delta^{A_2 B_2} \delta^{A_3 B_3} D_{n;st}^{a_1 \bar{b}_2} D_{n;st}^{\bar{b}_1 a_2} D_{n;st}^{\bar{b}_1 \bar{b}_2 a_3} \\ & - \delta^{A_1 B_2} \delta^{A_2 B_1} \delta^{A_3 B_3} D_{n;st}^{a_2 \bar{b}_2} D_{n;st}^{\bar{b}_1 a_1} D_{n;st}^{\bar{b}_1 \bar{b}_2 a_3} \\ & - \delta^{A_1 B_3} \delta^{A_2 B_2} \delta^{A_3 B_1} D_{n;st}^{a_3 \bar{b}_2} D_{n;st}^{\bar{b}_1 a_2} D_{n;st}^{\bar{b}_1 \bar{b}_2 a_1} \\ & - \delta^{A_1 B_1} \delta^{A_2 B_3} \delta^{A_3 B_2} D_{n;st}^{a_1 \bar{b}_2} D_{n;st}^{\bar{b}_1 a_3} D_{n;st}^{\bar{b}_1 \bar{b}_2 a_2} \\ & + \delta^{A_1 B_2} \delta^{A_2 B_3} \delta^{A_3 B_1} D_{n;st}^{a_3 \bar{b}_2} D_{n;st}^{\bar{b}_1 a_1} D_{n;st}^{\bar{b}_1 \bar{b}_2 a_2} \\ & + \delta^{A_1 B_3} \delta^{A_2 B_1} \delta^{A_3 B_2} D_{n;st}^{a_2 \bar{b}_2} D_{n;st}^{\bar{b}_1 a_3} D_{n;st}^{\bar{b}_1 \bar{b}_2 a_1} \end{aligned} \right) \quad (\text{B.28})$$

which in the single-flavor case (5.2) reduces to

$$(A_n)_{(q\bar{q})^3}^{\text{NMHV}} = \frac{\delta^{(4)}(p) \text{sign}(\tau)}{\langle 1 2 \rangle \dots \langle n 1 \rangle} \sum_{1 < s < t < n} \tilde{R}_{n;st} \left(D_{n;st}^{\bar{b}_1 \bar{b}_2} \right)^3 D_{n;st}^{a_1 a_2 a_3}. \quad (\text{B.29})$$

These simplified expressions are implemented in `GGT` by the functions `GGTnmhv6fermS` for the single-flavor case and `GGTnmhv6ferm` for the general-flavor case. See appendix C for the documentation.

B.3 N²MHV amplitudes

B.3.1 Two fermions

We continue the list of quark-gluon amplitudes by applying the master formulas (5.2) and (6.2) in the N²MHV case with up to six fermions. The amplitude with three negative-helicity gluons

at positions c_1, c_2, n , a quark at position a and an anti-quark at position \bar{b} , is

$$(A_n)_{(q\bar{q})}^{N^2\text{MHV}} = \frac{\delta^{(4)}(p) \text{sign}(\tau)}{\langle 1 2 \rangle \dots \langle n 1 \rangle} \sum_{2 \leq a_1 < b_1 < n} \tilde{R}_{n;a_1 b_1} \cdot \left[\sum_{a_1+1 \leq a_2 < b_2 \leq b_1} \tilde{R}_{n;b_1 a_1; a_2 b_2}^{0;a_1 b_1} \cdot D_1^{c_1 c_2 a} \left(D_1^{c_1 c_2 \bar{b}} \right)^3 \right. \\ \left. + \sum_{b_1 \leq a_2 < b_2 < n} \tilde{R}_{n;a_2 b_2}^{a_1 b_1; 0} \cdot D_2^{c_1 c_2 a} \left(D_2^{c_1 c_2 \bar{b}} \right)^3 \right], \quad (\text{B.30})$$

with the 3×3 determinants D_1^{abc} and D_2^{abc} from eqs. (A.6) and (A.7).

B.3.2 Four fermions

For the amplitude with two negative-helicity gluons at positions c, n , as well as quarks and anti-quarks at positions $\alpha_1^{A_1}, \alpha_2^{A_2}$ and $\bar{\beta}_1^{B_1}, \bar{\beta}_2^{B_2}$, we obtain

$$(A_n)_{(q\bar{q})^2}^{N^2\text{MHV}} = \frac{\delta^{(4)}(p) \text{sign}(\tau)}{\langle 1 2 \rangle \dots \langle n 1 \rangle} \sum_{2 \leq a_1 < b_1 < n} \tilde{R}_{n;a_1 b_1} \times \\ \times \left[\sum_{a_1 < a_2 < b_2 \leq b_1} \tilde{R}_{n;b_1 a_1; a_2 b_2}^{0;a_1 b_1} \left(D_1^{c \bar{\beta}_1 \bar{\beta}_2} \right)^2 \left(\delta_{A_1}^{B_1} \delta_{A_2}^{B_2} D_1^{c \alpha_1 \bar{\beta}_2} D_1^{c \bar{\beta}_1 \alpha_2} - \delta_{A_1}^{B_2} \delta_{A_2}^{B_1} D_1^{c \alpha_2 \bar{\beta}_2} D_1^{c \bar{\beta}_1 \alpha_1} \right) \right. \\ \left. + \sum_{b_1 \leq a_2 < b_2 < n} \tilde{R}_{n;a_2 b_2}^{a_1 b_1; 0} \left(D_2^{c \bar{\beta}_1 \bar{\beta}_2} \right)^2 \left(\delta_{A_1}^{B_1} \delta_{A_2}^{B_2} D_2^{c \alpha_1 \bar{\beta}_2} D_2^{c \bar{\beta}_1 \alpha_2} - \delta_{A_1}^{B_2} \delta_{A_2}^{B_1} D_2^{c \alpha_2 \bar{\beta}_2} D_2^{c \bar{\beta}_1 \alpha_1} \right) \right] \quad (\text{B.31})$$

in the $\mathcal{N} = 4$ super Yang-Mills case, and

$$(A_n)_{(q\bar{q})^2}^{N^2\text{MHV}} = \frac{\delta^{(4)}(p) \text{sign}(\tau)}{\langle 1 2 \rangle \dots \langle n 1 \rangle} \sum_{2 \leq a_1 < b_1 < n} \tilde{R}_{n;a_1 b_1} \cdot \left[\sum_{a_1 < a_2 < b_2 \leq b_1} \tilde{R}_{n;b_1 a_1; a_2 b_2}^{0;a_1 b_1} \cdot D_1^{c \alpha_1 \alpha_2} \left(D_1^{c \bar{\beta}_1 \bar{\beta}_2} \right)^3 \right. \\ \left. + \sum_{b_1 \leq a_2 < b_2 < n} \tilde{R}_{n;a_2 b_2}^{a_1 b_1; 0} \cdot D_2^{c_1 c_2 a} \left(D_2^{c_1 c_2 \bar{b}} \right)^3 \right] \quad (\text{B.32})$$

for single-flavor QCD.

B.3.3 Six fermions

For the $\mathcal{N} = 4$ super Yang-Mills amplitude with one negative-helicity gluon at position n , quarks and anti-quarks at positions $\alpha_1^{A_1}, \alpha_2^{A_2}, \alpha_3^{A_3}$ and $\bar{\beta}_1^{B_1}, \bar{\beta}_2^{B_2}, \bar{\beta}_3^{B_3}$, our master formula yields

$$(A_n)_{(q\bar{q})^3}^{N^2\text{MHV}} = \frac{\delta^{(4)}(p) \text{sign}(\tau)}{\langle 1 2 \rangle \dots \langle n 1 \rangle} \sum_{2 \leq a_1 < b_1 < n} \tilde{R}_{n;a_1 b_1} \times$$

$$\begin{aligned}
& \times \left[\sum_{a_1 < a_2 < b_2 \leq b_1} \tilde{R}_{n; b_1 a_1; a_2 b_2}^{0; a_1 b_1} D_1^{\bar{\beta}_1 \bar{\beta}_2 \bar{\beta}_3} \left(\delta_{A_1}^{B_1} \delta_{A_2}^{B_2} \delta_{A_3}^{B_3} D_1^{\alpha_1 \bar{\beta}_2 \bar{\beta}_2} D_1^{\bar{\beta}_1 \alpha_2 \bar{\beta}_2} D_1^{\bar{\beta}_2 \bar{\beta}_2 \alpha_3} \pm \text{permutations of } \left\{ \begin{matrix} A_i \\ \alpha_i \end{matrix} \right\} \right) \right. \\
& \quad \left. + \sum_{b_1 \leq a_2 < b_2 < n} \tilde{R}_{n; a_2 b_2}^{a_1 b_1; 0} D_2^{\bar{\beta}_1 \bar{\beta}_2 \bar{\beta}_3} \left(\delta_{A_1}^{B_1} \delta_{A_2}^{B_2} \delta_{A_3}^{B_3} D_2^{\alpha_1 \bar{\beta}_2 \bar{\beta}_2} D_2^{\bar{\beta}_1 \alpha_2 \bar{\beta}_2} D_2^{\bar{\beta}_2 \bar{\beta}_2 \alpha_3} \pm \text{permutations of } \left\{ \begin{matrix} A_i \\ \alpha_i \end{matrix} \right\} \right) \right], \tag{B.33}
\end{aligned}$$

which in the single-flavor case simplifies to

$$\begin{aligned}
(A_n)_{(q\bar{q})^3}^{\text{N}^2\text{MHV}} &= \frac{\delta^{(4)}(p) \text{sign}(\tau)}{\langle 1 2 \rangle \dots \langle n 1 \rangle} \sum_{2 \leq a_1 < b_1 < n} \tilde{R}_{n; a_1 b_1} \cdot \left[\sum_{a_1 < a_2 < b_2 \leq b_1} \tilde{R}_{n; b_1 a_1; a_2 b_2}^{0; a_1 b_1} D_1^{\alpha_1 \alpha_2 \alpha_3} \left(D_1^{\bar{\beta}_1 \bar{\beta}_2 \bar{\beta}_3} \right)^3 \right. \\
& \quad \left. + \sum_{b_1 \leq a_2 < b_2 < n} \tilde{R}_{n; a_2 b_2}^{a_1 b_1; 0} D_2^{\alpha_1 \alpha_2 \alpha_3} \left(D_2^{\bar{\beta}_1 \bar{\beta}_2 \bar{\beta}_3} \right)^3 \right]. \tag{B.34}
\end{aligned}$$

We recall that these formulas hold for arbitrary color-orderings of the n partons.

We have implemented all of the above simplified expressions for NNMHV amplitudes with up to six fermions in the functions `GGTnnmhv2ferm`, `GGTnnmhv4ferm`, `GGTnnmhv6ferm` in the `GGT` package.

C The Mathematica package GGT

Here we describe the Mathematica package `GGT` (gluon-gluino trees) provided with the [arXiv.org](http://arxiv.org) submission of the present paper and also accessible via <http://qft.physik.hu-berlin.de>.

The idea is to provide the formulas derived in the present paper in computer-readable form, such that the interested reader can use them without having to type them in. We have also included a simple numerical evaluation routine for given phase-space points in the `GGT` package, as well as an interface to the spinor-helicity package `SOM` [42]. The issue of computer speed optimization will be commented upon below.

Let us now describe the different functions in `GGT` and then give a specific example. The following functions are provided in `GGT`

- `GGTgluon[n, H]`
gives the n -gluon amplitude (4.2), with the positions of the negative-helicity gluons given by the list `H`.
- `GGTfermionS[n, gluonlist, fermlist, afermlist]`
gives the n -parton amplitude (5.2) of an arbitrary number of gluons and single-flavor fermion/antifermions. The positions of the negative-helicity gluons, helicity $+\frac{1}{2}$ fermions, and helicity $-\frac{1}{2}$ anti-fermions are given by the lists `gluonlist`, `fermlist`, and `afermlist`, respectively.

- `GGTfermion[n, gluonlist, fermlist, afermlist]`
is the generalization of `GGTfermionS` to multiple fermion flavors, eq. (6.2). The positions of the negative-helicity gluons are given by the list `gluonlist`. The positions q_i, \bar{q}_i and flavors A_i, B_i of the helicity $+\frac{1}{2}$ fermions and helicity $-\frac{1}{2}$ anti-fermions are given by the lists `fermlist` = $\{\{q_i, A_i\}, \dots\}$, and `afermlist` = $\{\{\bar{q}_i, A_i\}, \dots\}$, respectively.
- `GGTsuperamp[n, k]`
is the N^k MHV superamplitude of n superfields, with the MHV superamplitude factored out, in terms of the R invariants.

Let us give an example. We can load the `GGT` package using

```
<< GGT.m
```

Suppose we want to evaluate a gluon amplitude. Typing

```
GGTgluon[6, {3, 5, 6}]
```

prints the 6-gluon NMHV amplitude with helicity configuration $++-+--$,

$$\frac{1}{\langle 1|2\rangle\langle 2|3\rangle\langle 3|4\rangle\langle 4|5\rangle\langle 5|6\rangle\langle 6|1\rangle} \left(\frac{\langle 2|1\rangle\langle 4|3\rangle (s_{2,4}\langle 6|3\rangle\langle 6|5\rangle + \langle 6|x_{6,4}|x_{4,2}|3\rangle\langle 6|5\rangle)^4}{s_{2,4}\langle 6|x_{6,2}|x_{2,4}|3\rangle\langle 6|x_{6,2}|x_{2,4}|4\rangle\langle 6|x_{6,4}|x_{4,2}|1\rangle\langle 6|x_{6,4}|x_{4,2}|2\rangle} + \frac{\langle 2|1\rangle\langle 5|4\rangle (s_{2,5}\langle 6|3\rangle\langle 6|5\rangle\langle 6|x_{6,5}|x_{5,2}|3\rangle\langle 6|5\rangle)^4}{s_{2,5}\langle 6|x_{6,2}|x_{2,5}|4\rangle\langle 6|x_{6,2}|x_{2,5}|5\rangle\langle 6|x_{6,5}|x_{5,2}|1\rangle\langle 6|x_{6,5}|x_{5,2}|2\rangle} + \frac{\langle 3|2\rangle\langle 5|4\rangle (s_{3,5}\langle 6|3\rangle\langle 6|5\rangle + \langle 6|x_{6,5}|x_{5,3}|3\rangle\langle 6|5\rangle)^4}{s_{3,5}\langle 6|x_{6,3}|x_{3,5}|4\rangle\langle 6|x_{6,3}|x_{3,5}|5\rangle\langle 6|x_{6,5}|x_{5,3}|2\rangle\langle 6|x_{6,5}|x_{5,3}|3\rangle} \right)$$

`GGT` formatted the output for better readability. The underlying formula, which can be accessed explicitly, *e.g.* by using `Inputform[...]`, depends on the following quantities: The spinor products $\langle ij \rangle$ are denoted by `GGTspaa[i, j]`. Differences between dual coordinates $x_{i,j} = p_i + p_{i+1} + \dots + p_{j-1}$ are denoted by `GGTx[i, j]`. Finally, the abbreviation $x_{ij}^2 = s_{i,j-1}$ is used and denoted by `GGTs[i, j-1]`.

In order to obtain numerical values, we can use the spinor-helicity package `SOM` [42]. The function `GGTtoSpinors` converts the expression into one that can be evaluated by the latter package. In our example, the commands

```
<< Spinors.m
GenMomenta[1, 2, 3, 4, 5, 6]
```

load the `SOM` package and use one of its functions to generate arbitrary momenta for a six-particle scattering process. Finally, numerical values of the amplitude at that phase-space point can be obtained by the command

```
GGTtoSpinors[GGTgluon[6, {3, 5, 6}]] //N
```

A faster implementation for the numerical evaluation of the `GGT` formulas is provided by the function `GGTgenvar[P]` which generates the spinors and region momenta for a numerical evaluation of an amplitude at a desired phase-space point $P = \{p_1, p_2, \dots, p_n\}$. For example, for the kinematic point given in eq. (4.6) of ref. [43] (which to save space we give here to only three significant digits), one would use

```
GGTgenvar[{{{-3.0, 2.12, 1.06, 1.84}, {-3.0, -2.12, -1.06, -1.84}, {2.0, 2.0, 0.0, 0.0},
{0.857, -0.316, 0.797, 0.0}, {1.0, -0.184, 0.465, 0.866}, {2.14, -1.5, -1.26, -0.866}}}]
```

One can then evaluate an amplitude numerically by the command

```
GGTnumeric[GGTfermionS[6, {1, 6}, {2, 4}, {3, 5}]]
- 0.496838 + 0.0714737 i
```

This approach is considerably faster than the `GGTtoSpinors[...]/N` function discussed above.

Let us comment about the evaluation time needed using our approach. It is clear that for any serious applications or for comparisons with other methods, one should implement our analytical formulas using a low-level programming language, such as C, C++ or FORTRAN. For example, an implementation of the NMHV formulas in C++ results in a speedup of orders of magnitude over a similar implementation in Mathematica. Moreover, it is important to efficiently cache (store the numerical values of) quantities that are used repeatedly. In this spirit, the Mathematica demonstration package `GGT` provides a computer-readable version of the formulas needed for such an approach, so that the user does not have to type them in manually.

Our analytical formulas are very similar, and in some cases identical, to the ones obtained in a very recent paper [44]. The latter also correspond to solutions of the BCFW recursion relations, based on refs. [45], but may differ in form since they can correspond to different factorization channels. Another difference is that they are written using momentum-twistor variables [46]. Ref. [44] contains a numerical Mathematica implementation of these formulas. When the formulas of our paper and that of ref. [44] are both implemented with appropriate caching in C++, for the NMHV tree amplitudes for $Vq\bar{q}ggggg$ and $Vq\bar{q}Q\bar{Q}ggg$, their evaluation time is similar [47].

We remark that in approaches based on BCFW recursion relations, the asymptotic number of terms in $N^k\text{MHV}_n$ amplitudes as n becomes large is quadratic in n for NMHV, quartic for NNMHV and worse for higher k . This is the reason we especially simplified the NMHV and NNMHV formulas presented in our paper, since we expect that they will be the most useful for practical applications, especially for small n . For $k > 2$ and large n there are at least two efficient numerical strategies making use of these formulae. First, one could use our formulae as initial conditions for a numerical implementation of the BCFW recursion relations, as described in section 3. Alternatively, one could use the Berends-Giele approach for $k > 2$, implemented using an efficient caching, in combination with our formulas for $k \leq 2$ [48].

We also included further functions that evaluate directly the simplified amplitudes of Appendix A and B. They can be accessed via the following functions.

- $\text{GGTnmhvgluon}[n, a, b]$
is the simplified n -parton NMHV gluon amplitude with negative-helicity gluons at positions a, b and n .
- $\text{GGTnnmhvgluon}[n, a, b, c]$
is the simplified n -parton NNMHV gluon amplitude with negative-helicity gluons at positions a, b, c and n .
- $\text{GGTnmhv2ferm}[n, c, a, \bar{b}]$
is the simplified n -parton NMHV two-fermion amplitude with negative-helicity gluons at positions c, n and a fermion/anti-fermion at positions a and \bar{b} .
- $\text{GGTnnmhv2ferm}[n, c_1, c_2, a, \bar{b}]$
is the simplified n -parton NNMHV two-fermion amplitude with negative-helicity gluons at positions c_1, c_2 and n and a fermion/anti-fermion at position a and \bar{b} .
- $\text{GGTnmhv4ferm}[n, \{\{a_1, A_1\}, \{a_2, A_2\}\}, \{\{\bar{b}_1, B_1\}, \{\bar{b}_2, B_2\}\}]$
is the simplified n -parton NMHV four-fermion amplitude with a negative-helicity gluon at position n , two gluinos of flavors A_i at positions a_i and two anti-gluinos of flavors B_i at positions \bar{b}_i .
- $\text{GGTnmhv4fermS}[n, \{a_1, a_2\}, \{\bar{b}_1, \bar{b}_2\}]$
is the simplified n -parton NMHV four-fermion amplitude with a negative-helicity gluon at position n and equally flavored gluinos/anti-gluinos at positions a_i and \bar{b}_i , respectively.
- $\text{GGTnnmhv4ferm}[n, c, \{\{a_1, A_1\}, \{a_2, A_2\}\}, \{\{\bar{b}_1, B_1\}, \{\bar{b}_2, B_2\}\}]$
is the simplified n -parton NNMHV four-fermion amplitude with two negative-helicity gluons at position c, n , two gluinos of flavors A_i at positions a_i and two anti-gluinos of flavors B_i at positions \bar{b}_i .
- $\text{GGTnnmhv4fermS}[n, c, \{a_1, a_2\}, \{\bar{b}_1, \bar{b}_2\}]$
is the simplified n -parton NNMHV four-fermion amplitude with negative-helicity gluons at positions c, n and equally flavored gluinos/anti-gluinos at positions a_i and \bar{b}_i , respectively.
- $\text{GGTnmhv6ferm}[n, B_3, \{\{a_1, A_1\}, \{a_2, A_2\}, \{a_3, A_3\}\}, \{\{\bar{b}_1, B_1\}, \{\bar{b}_2, B_2\}\}]$
is the simplified n -parton NMHV six-fermion amplitude with three gluinos of flavors A_i at positions a_i and three anti-gluinos of flavors B_i at positions \bar{b}_i . Note that $\bar{b}_3 = n$.
- $\text{GGTnmhv6fermS}[n, \{a_1, a_2, a_3\}, \{\bar{b}_1, \bar{b}_2\}]$
is the simplified n -parton NMHV six-fermion amplitude with equally flavored gluinos/anti-gluinos at positions a_i and \bar{b}_i , respectively. Note that $\bar{b}_3 = n$.
- $\text{GGTnnmhv6ferm}[n, \{\{a_1, A_1\}, \{a_2, A_2\}, \{a_3, A_3\}\}, \{\{\bar{b}_1, B_1\}, \{\bar{b}_2, B_2\}, \{\bar{b}_3, B_3\}\}]$
is the simplified n -parton NNMHV six-fermion amplitude with a negative helicity gluon at position n and three gluinos of flavors A_i at positions a_i and three anti-gluinos of flavors B_i at positions \bar{b}_i .

- `GGTnmhv6fermS[n, {a1, a2, a3}, {b̄1, b̄2, b̄3}]`
is the simplified n -parton NNMHV six-fermion amplitude with a negative helicity gluon at position n and equally flavored gluinos/anti-gluinos at positions a_i and \bar{b}_i , respectively.

The full list of functions available in GGT can be obtained by typing

```
$GGTfunctions
```

along with the documentation of each implemented function that can be accessed via the command

```
?GGTgluon
```

for example.

References

- [1] T. Stelzer and W. Long, “Automatic generation of tree level helicity amplitudes”, *Comput.Phys.Commun.* 81, 357 (1994), [hep-ph/9401258](#). • J. Alwall et al., “*MadGraph/MadEvent v4: The New Web Generation*”, *JHEP* 0709, 028 (2007), [arxiv:0706.2334](#).
- [2] A. Pukhov et al., “*CompHEP: A Package for evaluation of Feynman diagrams and integration over multiparticle phase space*”, [hep-ph/9908288](#), user’s manual for version 33.
- [3] F. Krauss, R. Kuhn and G. Soff, “*AMEGIC++ 1.0: A Matrix element generator in C++*”, *JHEP* 0202, 044 (2002), [hep-ph/0109036](#).
- [4] F. A. Berends and W. T. Giele, “*Recursive Calculations for Processes with n Gluons*”, *Nucl. Phys.* B306, 759 (1988).
- [5] T. Gleisberg and S. Höche, “*Comix, a new matrix element generator*”, *JHEP* 0812, 039 (2008), [arxiv:0808.3674](#).
- [6] F. Caravaglios and M. Moretti, “*An algorithm to compute Born scattering amplitudes without Feynman graphs*”, *Phys.Lett.* B358, 332 (1995), [hep-ph/9507237](#). • F. Caravaglios, M. L. Mangano, M. Moretti and R. Pittau, “*A New approach to multijet calculations in hadron collisions*”, *Nucl.Phys.* B539, 215 (1999), [hep-ph/9807570](#).
- [7] A. Kanaki and C. G. Papadopoulos, “*HELAC: A Package to compute electroweak helicity amplitudes*”, *Comput.Phys.Commun.* 132, 306 (2000), [hep-ph/0002082](#). • A. Cafarella, C. G. Papadopoulos and M. Worek, “*Helac-Phegas: A Generator for all parton level processes*”, *Comput.Phys.Commun.* 180, 1941 (2009), [arxiv:0710.2427](#).
- [8] M. Moretti, T. Ohl and J. Reuter, “*O’Mega: An Optimizing matrix element generator*”, [hep-ph/0102195](#). • W. Kilian, T. Ohl and J. Reuter, “*WHIZARD: Simulating Multi-Particle Processes at LHC and ILC*”, [arxiv:0708.4233](#).
- [9] S. J. Parke and T. R. Taylor, “*Perturbative QCD Utilizing Extended Supersymmetry*”, *Phys. Lett.* B157, 81 (1985). • Z. Kunszt, “*Combined Use of the Calkul Method and $N=1$ Supersymmetry to Calculate QCD Six Parton Processes*”, *Nucl. Phys.* B271, 333 (1986).

- [10] M. T. Grisaru, H. Pendleton and P. van Nieuwenhuizen, “*Supergravity and the S Matrix*”, Phys.Rev. D15, 996 (1977). • M. T. Grisaru and H. Pendleton, “*Some Properties of Scattering Amplitudes in Supersymmetric Theories*”, Nucl.Phys. B124, 81 (1977).
- [11] S. J. Parke and T. R. Taylor, “*An Amplitude for n Gluon Scattering*”, Phys. Rev. Lett. 56, 2459 (1986).
- [12] V. P. Nair, “*A current algebra for some gauge theory amplitudes*”, Phys. Lett. B214, 215 (1988).
- [13] Z. Bern, L. J. Dixon, D. C. Dunbar and D. A. Kosower, “*One-Loop n-Point Gauge Theory Amplitudes, Unitarity and Collinear Limits*”, Nucl. Phys. B425, 217 (1994), hep-ph/9403226.
- [14] Z. Bern, L. J. Dixon, D. C. Dunbar and D. A. Kosower, “*Fusing gauge theory tree amplitudes into loop amplitudes*”, Nucl. Phys. B435, 59 (1995), hep-ph/9409265.
- [15] Z. Bern, L. J. Dixon and D. A. Kosower, “*On-Shell Methods in Perturbative QCD*”, Annals Phys. 322, 1587 (2007), arxiv:0704.2798. • C. F. Berger and D. Forde, “*Multi-Parton Scattering Amplitudes via On-Shell Methods*”, arxiv:0912.3534.
- [16] E. Witten, “*Perturbative gauge theory as a string theory in twistor space*”, Commun. Math. Phys. 252, 189 (2004), hep-th/0312171.
- [17] R. Britto, F. Cachazo and B. Feng, “*New recursion relations for tree amplitudes of gluons*”, Nucl. Phys. B715, 499 (2005), hep-th/0412308. • R. Britto, F. Cachazo, B. Feng and E. Witten, “*Direct proof of tree-level recursion relation in Yang-Mills theory*”, Phys. Rev. Lett. 94, 181602 (2005), hep-th/0501052.
- [18] R. Britto, B. Feng, R. Roiban, M. Spradlin and A. Volovich, “*All split helicity tree-level gluon amplitudes*”, Phys. Rev. D71, 105017 (2005), hep-th/0503198.
- [19] N. Arkani-Hamed, F. Cachazo, C. Cheung and J. Kaplan, “*A Duality For The S Matrix*”, JHEP 1003, 020 (2010), arxiv:0907.5418.
- [20] M. Bianchi, H. Elvang and D. Z. Freedman, “*Generating Tree Amplitudes in $\mathcal{N} = 4$ SYM and $\mathcal{N} = 8$ SG*”, JHEP 0809, 063 (2008), arxiv:0805.0757.
- [21] J. M. Drummond and J. M. Henn, “*All tree-level amplitudes in $\mathcal{N} = 4$ SYM*”, JHEP 0904, 018 (2009), arxiv:0808.2475.
- [22] J. M. Drummond, J. Henn, G. P. Korchemsky and E. Sokatchev, “*Dual superconformal symmetry of scattering amplitudes in $\mathcal{N} = 4$ super-Yang-Mills theory*”, Nucl. Phys. B828, 317 (2010), arxiv:0807.1095.
- [23] A. Brandhuber, P. Heslop and G. Travaglini, “*A note on dual superconformal symmetry of the $\mathcal{N} = 4$ super Yang-Mills S-matrix*”, Phys. Rev. D78, 125005 (2008), arxiv:0807.4097.
- [24] J. M. Drummond, J. Henn, G. P. Korchemsky and E. Sokatchev, “*Generalized unitarity for $\mathcal{N} = 4$ super-amplitudes*”, arxiv:0808.0491.
- [25] J. M. Drummond, J. M. Henn and J. Plefka, “*Yangian symmetry of scattering amplitudes in $\mathcal{N} = 4$ super Yang-Mills theory*”, JHEP 0905, 046 (2009), arxiv:0902.2987.
- [26] J. Drummond, “*Hidden Simplicity of Gauge Theory Amplitudes*”, arxiv:1010.2418.
- [27] C. Berger et al., “*Precise Predictions for $W + 4$ Jet Production at the Large Hadron Collider*”, arxiv:1009.2338.

- [28] G. Ossola, C. G. Papadopoulos and R. Pittau, “Reducing full one-loop amplitudes to scalar integrals at the integrand level”, Nucl.Phys. B763, 147 (2007), hep-ph/0609007. • G. Ossola, C. G. Papadopoulos and R. Pittau, “CutTools: A Program implementing the OPP reduction method to compute one-loop amplitudes”, JHEP 0803, 042 (2008), arxiv:0711.3596. • G. Ossola, C. G. Papadopoulos and R. Pittau, “On the Rational Terms of the one-loop amplitudes”, JHEP 0805, 004 (2008), arxiv:0802.1876.
- [29] R. K. Ellis, W. Giele and Z. Kunszt, “A Numerical Unitarity Formalism for Evaluating One-Loop Amplitudes”, JHEP 0803, 003 (2008), arxiv:0708.2398.
- [30] W. T. Giele, Z. Kunszt and K. Melnikov, “Full one-loop amplitudes from tree amplitudes”, JHEP 0804, 049 (2008), arxiv:0801.2237. • W. Giele and G. Zanderighi, “On the Numerical Evaluation of One-Loop Amplitudes: The Gluonic Case”, JHEP 0806, 038 (2008), arxiv:0805.2152.
- [31] C. Berger et al., “An Automated Implementation of On-Shell Methods for One-Loop Amplitudes”, Phys.Rev. D78, 036003 (2008), arxiv:0803.4180.
- [32] Z. Bern and A. Morgan, “Massive loop amplitudes from unitarity”, Nucl.Phys. B467, 479 (1996), hep-ph/9511336. • Z. Bern, L. J. Dixon, D. C. Dunbar and D. A. Kosower, “One loop self-dual and $\mathcal{N} = 4$ super Yang-Mills”, Phys.Lett. B394, 105 (1997), hep-th/9611127. • C. Anastasiou, R. Britto, B. Feng, Z. Kunszt and P. Mastrolia, “D-dimensional unitarity cut method”, Phys.Lett. B645, 213 (2007), hep-ph/0609191. • R. Britto and B. Feng, “Integral coefficients for one-loop amplitudes”, JHEP 0802, 095 (2008), arxiv:0711.4284.
- [33] S. Badger, “Direct Extraction Of One Loop Rational Terms”, JHEP 0901, 049 (2009), arxiv:0806.4600.
- [34] Z. Bern, L. J. Dixon and D. A. Kosower, “Bootstrapping multi-parton loop amplitudes in QCD”, Phys.Rev. D73, 065013 (2006), hep-ph/0507005. • C. F. Berger, Z. Bern, L. J. Dixon, D. Forde and D. A. Kosower, “Bootstrapping One-Loop QCD Amplitudes with General Helicities”, Phys.Rev. D74, 036009 (2006), hep-ph/0604195.
- [35] L. F. Alday, J. M. Henn, J. Plefka and T. Schuster, “Scattering into the fifth dimension of $\mathcal{N} = 4$ super Yang-Mills”, JHEP 1001, 077 (2010), arxiv:0908.0684.
- [36] M. L. Mangano and S. J. Parke, “Multi-Parton Amplitudes in Gauge Theories”, Phys. Rept. 200, 301 (1991), hep-th/0509223.
- [37] Z. Bern, L. J. Dixon and D. A. Kosower, “One-loop amplitudes for $e^+ e^-$ to four partons”, Nucl. Phys. B513, 3 (1998), hep-ph/9708239.
- [38] M. Dinsdale, M. Ternick and S. Weinzierl, “A Comparison of efficient methods for the computation of Born gluon amplitudes”, JHEP 0603, 056 (2006), hep-ph/0602204.
- [39] G. Georgiou, E. W. N. Glover and V. V. Khoze, “Non-MHV Tree Amplitudes in Gauge Theory”, JHEP 0407, 048 (2004), hep-th/0407027.
- [40] D. Binosi and L. Theussl, “JaxoDraw: A Graphical user interface for drawing Feynman diagrams”, Comput.Phys.Commun. 161, 76 (2004), hep-ph/0309015. • D. Binosi, J. Collins, C. Kaufhold and L. Theussl, “JaxoDraw: A Graphical user interface for drawing Feynman diagrams. Version 2.0 release notes”, Comput.Phys.Commun. 180, 1709 (2009), arxiv:0811.4113.

- [41] J. Vermaseren, “*Axodraw*”, *Comput.Phys.Commun.* 83, 45 (1994).
- [42] D. Maitre and P. Mastrolia, “*S@M, a Mathematica Implementation of the Spinor-Helicity Formalism*”, *Comput. Phys. Commun.* 179, 501 (2008), [arxiv:0710.5559](#).
- [43] R. K. Ellis, W. Giele and G. Zanderighi, “*The One-loop amplitude for six-gluon scattering*”, *JHEP* 0605, 027 (2006), [hep-ph/0602185](#).
- [44] J. L. Bourjaily, “*Efficient Tree-Amplitudes in $N=4$: Automatic BCFW Recursion in Mathematica*”, [arxiv:1011.2447](#).
- [45] N. Arkani-Hamed, F. Cachazo, C. Cheung and J. Kaplan, “*The S-Matrix in Twistor Space*”, [arxiv:0903.2110](#). • J. L. Bourjaily, J. Trnka, A. Volovich and C. Wen, “*The Grassmannian and the Twistor String: Connecting All Trees in $N=4$ SYM*”, [arxiv:1006.1899](#).
- [46] A. Hodges, “*Eliminating spurious poles from gauge-theoretic amplitudes*”, [arxiv:0905.1473](#). • L. Mason and D. Skinner, “*Dual Superconformal Invariance, Momentum Twistors and Grassmannians*”, *JHEP* 0911, 045 (2009), [arxiv:0909.0250](#).
- [47] Z. Bern, H. Ita and K. Ozeren, private communication.
- [48] P. Uwer and B. Biedermann, private communication.